AN EXAMINATION OF THE EFFECTS OF MITOCHONDRIAL TRANSPORT DISRUPTION IN CORTICAL NEURONS AND ASTROCYTES

by

Justin James Torres Lardizabal
Associate's Certificate, British Columbia Institute of Technology, 2006
BSc, University of British Columbia, 2005

THESIS SUBMITTED IN PARTIAL FULFILLMENT OF
THE REQUIREMENTS FOR THE DEGREE OF

MASTER OF SCIENCE

In the
Department of Biological Sciences

SIMON FRASER UNIVERSITY

Spring 2010

APPROVAL

Name: Justin James Torres Lardizabal

Degree: Master of Science

Title of Thesis:

An Examination of the Effects of Mitochondrial Transport Disruption in Cortical Neurons and Astrocytes

Examining Committee:

Chair: Dr. B. Roitberg, Professor

Dr. Dr. G. Rintoul, Assistant Professor, Senior Supervisor
Department of Biological Sciences, S.F.U.

Dr. M. Silverman, Assistant Professor
Department of Biological Sciences, S.F.U.

Dr. C. Krieger, Professor
Department of Biomedical Physiology and Kinesiology, S.F.U.,
Public Examiner

9 February 2010
Date Approved

Declaration of
Partial Copyright Licence

SFU SIMON FRASER UNIVERSITY
THINKING OF THE WORLD

STATEMENT OF ETHICS APPROVAL

The author, whose name appears on the title page of this work, has obtained, for the research described in this work, either:

(a) Human research ethics approval from the Simon Fraser University Office of Research Ethics,

or

(b) Advance approval of the animal care protocol from the University Animal Care Committee of Simon Fraser University;

or has conducted the research

(c) as a co-investigator, collaborator or research assistant in a research project approved in advance,

or

(d) as a member of a course approved in advance for minimal risk human research, by the Office of Research Ethics.

A copy of the approval letter has been filed at the Theses Office of the University Library at the time of submission of this thesis or project.

The original application for approval and letter of approval are filed with the relevant offices. Inquiries may be directed to those authorities.

Simon Fraser University Library
Simon Fraser University
Burnaby, BC, Canada

Last update: Spring 2010

ABSTRACT

Recent studies have revealed that mitochondria are mobile structures within neurons and are transported by molecular motors associated with the cytoskeleton. The significance of mitochondrial motility is unknown although it may be connected to intracellular ATP distribution and/or calcium sequestration. Therefore, disrupted mitochondrial translocation may compromise these functions and contribute to neuronal injury. In this study we inhibited mitochondrial trafficking by disrupting the dynactin complex and observed the effects on mitochondrial dynamics. In comparison to control cells, mitochondria were smaller and were largely absent from peripheral regions of astrocytes and the amount of mitochondrial movement exhibited by transport-disrupted cells was severely diminished. Calcium uptake and mitochondrial membrane potential were also significantly reduced. Cell survival after glutamate challenge was unaffected. These studies give us some insight into the importance of mitochondrial transport in neuronal health.

Keywords:
Primary Cortical neurons
Mitochondria
Molecular motors
Calcium homeostasis
Membrane potential
Organelle transport
CC1
Dynactin

ACKNOWLEDGEMENTS

I want to express my deepest appreciation and thanks to all of those that helped make this possible. Most of all, I would like to thank my senior supervisor, Dr. Gordon Rintoul, for his guidance, wisdom, patience, encouragement, and understanding in the lab and in life. I would also like to thank Dr. Michael Silverman for agreeing to be on my supervisory committee and for his feedback and guidance in the project and to Dr. Charles Krieger, my external examiner for his input, advice, and interest in my project. Thank you to Audrey Speelman for providing me with the tools and techniques and the patience needed to complete my project. My thanks go out to the past and present members of the Rintoul lab for making my experience even more enjoyable. I would like to thank my friends and family for their love and support throughout my stay at SFU. Finally, I would like to thank the loves of my life, Celine and Joseph their unconditional love and support through thick and thin. Thank you all so much.

TABLE OF CONTENTS

LIST OF FIGURES

LIST OF ABBREVIATIONS

ΔΨm	mitochondrial membrane potential
ATP	Adenosine Triphosphate
AUC	area under the curve
BSA	bovine serum albumin
BDNF	brain-derived neurotrophic factor
$[Ca^{+2}]_i$	intracellular calcium
CC1	first coiled-coil
CC2	second coiled-coil
CFP	cyan fluorescent protein
DIV	days *in vitro*
DNM1L	dynamin 1-like protein
Drp1	dynamin-related protein
dHBSS	dissection HBSS
F_o	baseline fluorescence
F_f	final fluorescence
ΔF	change in fluorescence
FCCP	*p*-trifluoromethoxy-phenylhydrazone
GFP	green fluorescent protein
GRIF1	γ-aminobutyric acid A receptor-interacting factor-1
HBSS	Hepes buffered saline solution
HAP-1	Huntington Associated Protein 1
htt	huntingtin protein
KBP	KIF1 binding protein
KHC	kinesin heavy chain
KLC	kinesin light chain
LF 2000	Lipofectamine 2000
MAPs	microtubule-associated proteins
mPT	mitochondrial permeability transition
Mfn1	mitofusin-1
Mfn2	mitofusin-2
mt-eYFP	mitochondrial-targetted enhanced fluorescent protein
mtSOD1	copper-zinc superoxide dismutase mutant
NB	Neurobasal
NB-AO	neurobasal without antioxidants
NB+AO	neurobasal with antioxidants
NPY	neuropeptide Y
NMDA	N-methyl-D-aspartate
OIP106	O-linked *N*-acetylglucosamine-interacting protein 106
OPA1	optic atrophy protein 1

ROS	reactive oxygen species
SEM	standard error of the mean
TMRM	tetramethylrhodamine methyl ester

1 INTRODUCTION

The nervous system is an essential part of any living organism that coordinates and controls many activities of the body. Activities essential for survival such as movement, nutrient circulation, and ion balance are all controlled by the brain. The components that comprise the nervous system and allow its functions to be carried out are neurons and glia. Neurons are highly polarized cells that communicate signals in the form of action potentials with each other and to their innervated tissues. Glial cells are responsible for the maintenance and support of the neurons.

The morphology of a typical neuron is very unique in comparison to other cell types and consists of three main regions: a highly branched network of dendrites which receive input from other cells, the cell body or soma which processes the incoming signal and formulates the appropriate response, and the axon which transmits the cellular response to the intended target cells or tissue. Even within neurons, as in any biological system, there is a large amount of variation in neuronal morphology in different areas of the brain that are responsible for different functions. Differing morphologies of neurons arise in response to differing cellular needs.

Not only is there morphological polarity in neurons, but neurons exhibit polarity of protein expression and location and physiological processes as well. Due to the different demands of the dendrites versus the axon, the distribution of proteins, cytoskeletal elements, and biochemical processes that occur are very unique. Dendrites receive and transduce incoming signals from other cells and express many ligand receptors and ion channels that permit cell-to-cell communication to occur. Axons, on the other hand, transmit signals from the cell body to the presynaptic terminals and the transmission of these signals is accomplished using an entirely different set of proteins. The distribution of these proteins is highly specific and a complex control and sorting mechanism is needed to establish this polarity.

Neurons are highly specialized cells that control essential functions for an organism's health and survival. However, due to the highly specialized nature of neurons, if internal organelles and machinery do not perform their functions, then severe consequences to health can ensue. There are numerous examples of neurodegenerative diseases where such failures of these processes have been implicated in the pathological mechanisms.

1.1 Mitochondria

There are many organelles in the neuron that contribute to cell maintenance and health in their own unique way. Mitochondria are one of these organelles and pivotal contributors not only to cell life, but to cell death as well (as reviewed by Hollenbeck and Saxton, 2005; Chang and Reynolds, 2006). They are dynamic organelles that provide energy for all biochemical processes within neurons, and any cell, to occur. The primary function, and most highly characterized, is the production of adenosine triphosphate (ATP) (as reviewed by Ligon and Steward, 2000; Duchen, 2004; Hollenbeck and Saxton, 2005). ATP provides the energy required for biochemical processes to occur, from protein synthesis to cytoskeletal motor force generation (as reviewed by Duchen, 2004). Although production of ATP is the primary function of mitochondria, it is not the sole function that mitochondria undertake. Mitochondria are also responsible for modulating and buffering intracellular calcium and sequestering apoptotic factors (as reviewed by Duchen, 2004). For this reason, mitochondria can be the initial instigators that begin a cascade leading to cell death if their normal function is disrupted.

Although mitochondria are important in normal cellular function as mentioned above, they can also contribute to mechanisms of neurodegeneration and cell death. One well characterized example of mitochondria's participation in cell death is glutamate-mediated excitotoxicity. Excessive glutamate stimulation lead to increased intracellular calcium and toxicity (Olney and de Gubareff, 1978); however, Stout, et al. (1998) discovered that in order for heightened glutamate stimulation to be toxic to the

cell, the entering calcium must be taken up by mitochondria. In this model, pathophysiological concentrations of glutamate, a common neurotransmitter used in the nervous system, induces a large influx of calcium into the cell through N-methyl-D-aspartate (NMDA) receptors, which subsequently leads to cell death (Choi, 1988). Although numerous mechanisms of calcium buffering are present, the large influx of calcium is partially buffered by the mitochondria and causes a halt to their movement (Rintoul et al., 2003). As the amount of calcium within mitochondria increases, the membrane potential across the inner mitochondrial membrane begins to dissipate (as reviewed by Budd and Nicholls, 1996; Duchen, 2004), resulting in a decrease in ATP production (White and Reynolds, 1996). This is a crucial event that occurs during the initial stages of calcium-mediated toxicity because it compromises the main driving force for ATP synthesis and the inability to generate ATP contributes to cell dysfunction. Once the mitochondrial membrane potential ($\Delta\Psi m$) has collapsed, mitochondria begin to release increased amounts of reactive oxygen species (ROS) and pro-apoptotic factors (as reviewed by Mattson, 2003), which eventually leads to cell death.

Mitochondria are hypothesized to be autonomous aerobically respiring bacteria that were engulfed by another eukaryotic cell and, through years of evolution, developed a symbiotic relationship with its host (as reviewed by Margulis and Bermudes, 1985). Their life cycle, however, from biogenesis to degradation within the cell, remains to be fully elucidated. It is widely accepted that the majority of mitochondria are synthesized in close proximity to the nucleus, are subsequently transported around the cell to exert their function, and finally returned to the cell body where they are degraded and recycled (as reviewed by Chang and Reynolds, 2006). As logical as this suggestion seems, there is little evidence to support it and the exact details of the mitochondrial life cycle of have yet to be documented.

Recently, many studies have shown that mitochondria are extremely dynamic and mobile organelles. It is widely accepted that mitochondria are highly mobile organelles and are transported to regions within the neuron that have high energy demand (as reviewed by Ligon and Steward, 2000; Hollenbeck and Saxton, 2005;

Zinsmaier et al., 2009). Areas such as axonal growth cones (Povlishock, 1976), synapses (Palay, 1956), nodes of Ranvier (Fabricius et al., 1993), myelination boundaries (Bristow et al., 2002), and distal locations of high protein synthesis (Martin et al., 1998) exhibit high metabolic demands; therefore, in order to meet these demands, a great deal of energy is expended to translocate mitochondria to these areas. Not only are mitochondria highly mobile structures, but they are also constantly undergoing fission and fusion (as reviewed by Liesa et al., 2009). The balance between fission and fusion, which is controlled by a specific set of proteins, determines the morphology of mitochondria and can change in response to different stimuli (as reviewed by Chang and Reynolds, 2006; Liesa et al., 2009; Rintoul and Reynolds, 2009). The exact mechanisms that control mitochondrial fission and fusion and its importance to cellular health are still unclear.

1.1.1 Mitochondrial Movement

Like many other organelles in the neuron, mitochondria are believed to be synthesized in the cell body, however, there are many portions of the cell that have high energy demands and are located far from the cell body (as reviewed by Hollenbeck and Saxton, 2005; Chang et al., 2006b; Rintoul and Reynolds, 2009). If the cell depended on the diffusion of ATP to supply those distant regions of high energy demand, cell functions would be compromised, resulting in degeneration because the ATP would not be able to reach those locations fast enough. Therefore, in order to meet this demand, mitochondria are actively transported to these areas (as reviewed by Hollenbeck and Saxton, 2005; Chang et al., 2006b; Rintoul and Reynolds, 2009). The distribution of mitochondria within the cell is also a dynamic process. Changes in mitochondrial distribution and transport can be affected by physiological events and environmental changes if the distribution of the energy demand is changed (as reviewed by Chang and Reynolds, 2006; Liesa et al., 2009; Rintoul and Reynolds, 2009). In addition, mitochondrial movement can differ between different cellular locations as well. Overly *et al.* (1996) and Ligon and Steward (2000) observed differences in the movement of

mitochondria between axons and dendrites. Within axons, mitochondria had longer run lengths (Ligon and Steward, 2000) and twice as many mobile mitochondria (Overly et al., 1996) when compared to the dendrites. This difference in movement may be linked to the differences in microtubule organization (Overly et al., 1996; Ligon and Steward, 2000). To transport mitochondria, or any cellular cargo, three different proteins are required: cytoskeletal elements that provide the 'tracks' for organelle transport, molecular motors that move cargoes along the cytoskeletal tracks, and motor-cargo linker proteins that connect the molecular motors to their specific organelles or cargoes.

1.1.1.1 Neuronal Cytoskeleton

The cytoskeleton plays an important role in not only providing structural support for the cell but also in the transport of cellular components and organelles from one region to another. The cytoskeleton is responsible for maintaining the unique shape and polarity of the neuron. In addition, the cytoskeleton is dynamic and constantly changing, allowing the cell to grow and change shape (as reviewed by Chevalier-Larsen and Holzbaur, 2006). In neurons, the cytoskeleton is comprised of three different types of filaments: actin filaments, intermediate filaments, and microtubules (as reviewed by Chevalier-Larsen and Holzbaur, 2006). Actin filaments consist of actin monomers that assemble into a flexible helical polymer and are usually arranged in bundles, forming a large network (as reviewed by Cingolani and Goda, 2008). In the developing cell, actin is primarily involved in axonal outgrowth and cell motility (Mallavarapu and Mitchison, 1999): however, in a mature cell actin is highly concentrated in pre- and post-synaptic terminals (Fifkova and Delay, 1982; Landis et al., 1988). Intermediate filaments, which are predominantly neurofilaments in mature neurons comprise of three different subunit polypeptides; NF-L, NF-M, and NF-H (Lee et al., 1993) and provide structural support for the axon (Cleveland et al., 1991). Microtubules consist of α-tubulin and β-tubulin dimers that polymerize to form a cylindrical filament with a 'minus'- and 'plus'-end where the α-tubulin and β-tubulin are exposed, respectively (as reviewed by Desai and Mitchison, 1997). In the developing neuron, microtubules provide the majority of

the structural support for the outgrowing axon and are in constant cycles of polymerization and depolymerization (as reviewed by Geraldo and Gordon-Weeks, 2009). Whereas, in the mature neuron, microtubules are less dynamic and are stabilized by microtubule-associated proteins (MAPs) (as reviewed by Desai and Mitchison, 1997). In neurons, microtubules are arranged in an organized fashion and differ between axons and dendrites (Burton and Paige, 1981; Baas et al., 1988). In axons, microtubules are arranged with their 'plus'-end oriented towards the periphery and their 'minus'-end oriented towards the cell body (Burton and Paige, 1981; Baas et al., 1988). In dendrites, however, the microtubules exhibit a more complex organization. In the distal dendrites, the microtubules exhibit a similar organization as the axon, with the 'plus'-ends directed away from the cell body (Burton and Paige, 1981; Baas et al., 1988); however, the orientation of microtubules in the proximal dendrites is mixed, with the 'plus'- and 'minus'-ends of the filament pointing towards and away from the cell body (Baas et al., 1988). All three of these filaments combine to make up the cytoskeletal network, however, microtubules are the tracks along which long distance mitochondrial transport occurs (Hollenbeck and Saxton, 2005; Zinsmaier et al., 2009). The molecular motors that transport mitochondria along microtubules are kinesins and dyneins (as reviewed by Hollenbeck and Saxton, 2005; Chevalier-Larsen and Holzbaur, 2006).

1.1.1.2 Kinesins

Kinesins (KIFs) are a large family of microtubule-based motor proteins with forty-five members in mice and humans (as reviewed by Miki et al., 2001) that are responsible for transporting cellular cargoes towards the 'plus'-end of the microtubule. Structurally, kinesins can take many shapes; however, their basic structure remains the same. All kinesins have a globular motor domain that is highly conserved across species and

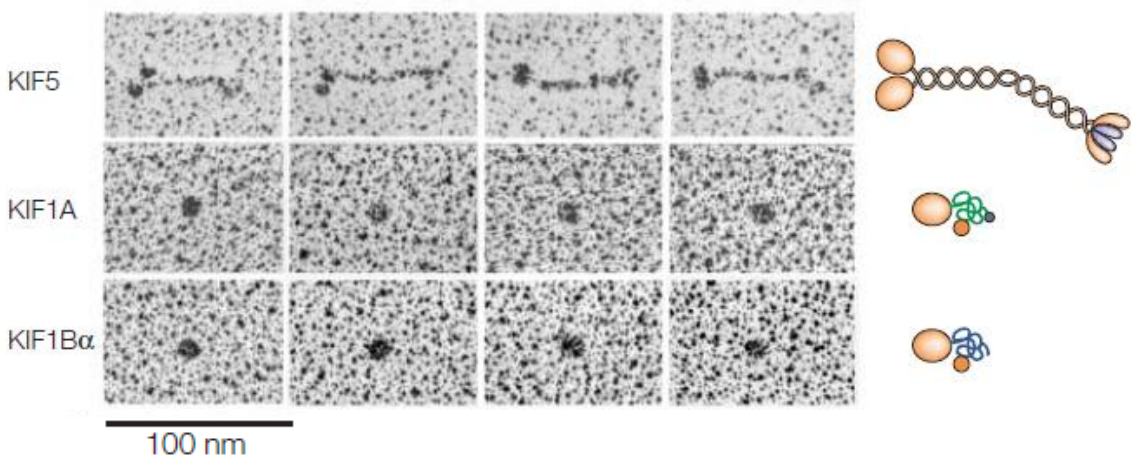

Figure 1.1: Kinesins and the variability of their structure.
Electron micrographs of different kinesins show their structure and the variability between family members. Diagrams, shown on the right, provide a sense of the interaction between the different subunits that make up the kinesin motor. KIF5 consists of kinesin heavy chains and kinesin light chains. KIF5 KHC's have a globular head responsible for motor activity and an α-helical central domain involved in dimerization. The C-termial domain of KIF5 KHC is interacts with KLC homodimers, forming a fan-like structure. KIF1A and KIF1B, however, are monomeric and globular. *(from Hirokawa and Takemura, 2005).*

consists of an ATP and a microtubule-binding sequence, but beyond the globular head each member has a different sequence, which is possibly involved in the cargo binding (as reviewed by Goldstein and Yang, 2000; Hirokawa and Takemura, 2005). Among all the different kinesin families, two are directly associated with mitochondria, KIF5 (Jellali et al., 1994) and KIF1Bα (Nangaku et al., 1994).

KIF5, or conventional kinesins/kinesin-1, has been the central focus of many investigations for many years and is responsible for 'plus'-end directed microtubule transport of mitochondria (Jellali et al., 1994). Its structure consists of kinesin heavy-chains (KHC) and kinesin light-chains (KLC) (See figure 1.1). In each KHC is an N-terminal globular motor domain which participates in motility and an alpha helical central domain which controls homodimerization (Hirokawa et al., 1989). The KLCs form homodimers and associate with the C-terminal domain of KHCs in a fan-like fashion, forming a hetero-tetramer (Diefenbach et al., 1998).

KIF1Bα is another kinesin that is linked to mitochondrial transport but is not nearly as well characterized as KIF5 (Nangaku et al., 1994). KIF1Bα is abundant in neurons and is part of the KIF1B family, or kinesin-3. KIF1Bα is a monomeric 'plus'-end directed motor that consists of an N-terminal globular motor domain and lacks the stalk and tail structure of KIF5 (Nangaku et al., 1994). Despite all the structural and functional differences between all the different members of the kinesins, they all require a motor-cargo linker protein that connects them to their cellular cargoes.

1.1.1.3 Adaptor Proteins Between Kinesins and Mitochondria

The exact mechanism that connects kinesins and their cargoes has yet to be determined, however, motor-cargo linker proteins that are specific to mitochondria were identified and extensively studied in recent years (see figure 1.3). Two *Drosophila* proteins, Miro and Milton, are involved in the process of linking KIF5 and mitochondria (Guo et al., 2005; Glater et al., 2006). Milton, along with its mammalian homologues γ-aminobutyric acid A receptor-interacting factor-1 (GRIF1) and O-linked *N*-acetylglucosamine-interacting protein 106 (OIP106), consist of two distinct motifs: coiled-coil domains and an N-terminal Huntington Associated Protein 1 (HAP-1) domain (Brickley et al., 2005; Glater et al., 2006). Previous co-immunoprecipitation experiments in *Drosophila* identified a direct link between Milton and the C-terminal end of kinesin heavy chain (Glater et al., 2006). In addition, Milton was also found to bind directly to Miro, which is an integral mitochondrial outer membrane protein that is a Rho-like GTPase containing two GTPase domains, two calcium-binding motifs, and a C-terminal membrane domain (Glater et al., 2006). Mutations in either Milton or Miro resulted in profound effects on mitochondria distribution and movement. Knockout mutations of *Drosophila* Miro or null mutants of Milton resulted in changes in mitochondrial distribution and reduced number mitochondria along the axon (Guo et al., 2005; Glater et al., 2006). Deletions of kinesin light chain, which does not appear to interact with either Milton or Miro, expectedly had no effect on the axonal transport of mitochondria

in *Drosophila* (Glater et al., 2006). Therefore, Miro and Milton link KIF5 to mitochondria and act independently from kinesin light chains.

Other proteins are reported to link mitochondria directly to kinesins but require further investigation. Proteins such as Kinectin (Ong et al., 2000), Syntabulin (Cai et al., 2005), and KIF1 binding protein (KBP) (Wozniak et al., 2005) have been associated with mitochondria and kinesins. Kinectins are a large family of proteins which possess 16 different isoforms (Santama et al., 2004). One kinectin isoform has been linked to mitochondria and various experiments that altered its endogenous expression yielded defects in mitochondrial distribution, implicating some contribution to mitochondrial trafficking (Santama et al., 2004). Syntabulin is a protein that is anchored to the outer mitochondrial membrane through a hydrophobic stretch of amino acids at the C-terminal end and interacts with the C-terminal end of KIF5 (Cai et al., 2005). Disruption of this interaction results in deficiencies in mitochondrial movement and trafficking (Cai et al., 2005). KBP is another mitochondrial motor-cargo linker protein that is reported to link mitochondria and KIF1Bα (Wozniak et al., 2005). Mutations and loss of KBP function appear to also affect mitochondrial distribution (Wozniak et al., 2005; Lyons et al., 2008). Dysfunction and mutations in these adaptor proteins clearly have a detrimental effect on mitochondrial trafficking. Although the linking mechanism between mitochondria and kinesin via adaptor proteins is becoming clearer, more research is warranted to further characterize the motor-cargo linker proteins that are involved specifically with mitochondria and motor proteins.

1.1.1.4 Dynein/Dynactin

Cytoplasmic dynein is another microtubule-based motor associated with mitochondria that does not possess nearly as much diversity as the kinesins but manages to control the vast majority of the transport directed to the cell body from the periphery in axons, or 'minus'-end directed transport in axons (Schnapp and Reese, 1989). Dynein is a large protein comprised of two heavy chains, and many intermediate, light intermediate, and light chains (as reviewed by Levy and Holzbaur, 2006). The heavy

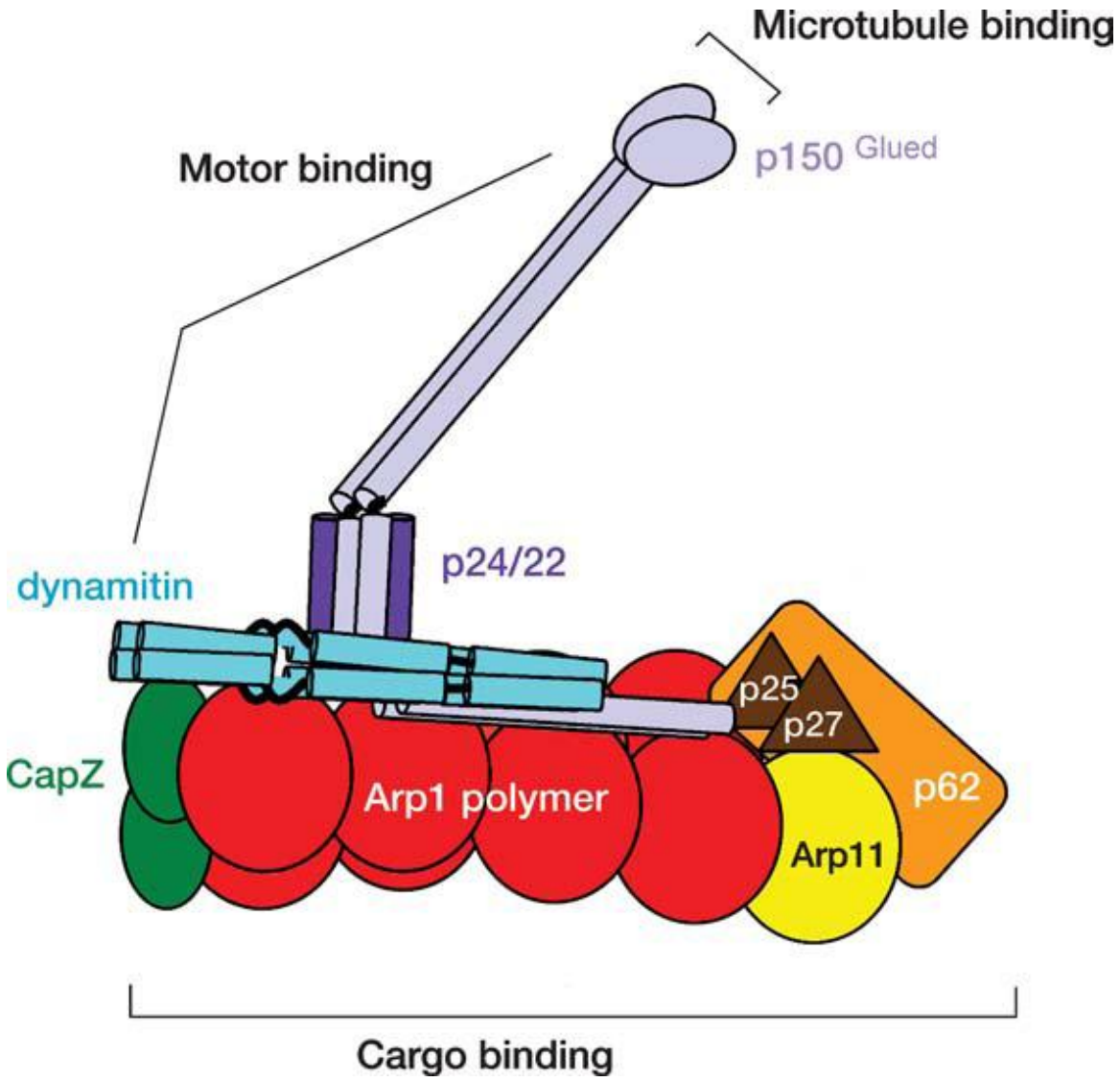

Figure 1.2: Dynactin and its subunits.
Dynactin consists of two distinct regions: the projecting arm and the Arp1 Rod. It is believed that the Arp1 rod is responsible for cargo interactions and the projecting arm is involved in motor and microtubule binding. The projecting arm consists of dynamitin, p24/22, and p150; while the Arp1 Rod is composed of a short filament (formed from Arp1 protein subunits) and capping proteins at each end of the filament. At one end, the capping protein p62 then binds p27and p25, which are hypothesized to regulate cargo interactions. *(from Shroer, 2004)*.

chains, which are involved in force production and microtubule binding, form globular motor heads and N-terminal flexible stalks that are involved in heavy chain dimerization (Habura et al., 1999) and interact with the intermediate (Habura et al., 1999) and light intermediate chains (Hughes et al., 1995). The globular head possess many AAA domain repeats (Mocz and Gibbons, 2001) forming a ring (Samso et al., 1998) which has a stalk that protrudes and binds to microtubules (Gee et al., 1997). Although dynein alone can generate force and move along microtubules, it cannot bind and transport organelles and cellular cargoes on its own and requires dynactin to act as an motor-cargo linker protein between dynein and its cargo (as reviewed by Schroer, 2004; Levy and Holzbaur, 2006).

Dynactin on its own is a large complex that consists of eleven unique proteins (see figure 1.2) (as reviewed by Schroer, 2004). The dynactin complex can be subdivided into two different regions: the Arp1 rod and the projecting arm (as reviewed by Quintyne and Schroer, 2002; Schroer, 2004). The Arp1 rod forms at the base of the complex and resembles a short actin-like filament, which is formed from the limited polymerization of the Arp1 protein; an actin related protein (Schafer et al., 1994; Bingham and Schroer, 1999). At each end of the filament is a capping protein; CapZ at one end (Schafer et al., 1994) and Arp11 (Eckley et al., 1999) and p62 at the other end (Schafer et al., 1994). In addition, p62 subunit associates with the p27 and p25 subunits, completing the Arp1 rod (Eckley et al., 1999). The projecting arm consists of three different subunits: $p150^{Glued}$, dynamitin, and p24/p22 (as reviewed by Schroer, 2004). The $p150^{Glued}$ subunit is the largest subunit of the dynactin complex and binds to microtubules and cytoplasmic dynein (Waterman-Storer et al., 1995; King et al., 2003). Each $p150^{Glued}$ subunit is an elongated homodimer of the $p150^{Glued}$ protein which has two N-terminal globular heads and two α-helical coiled-coil domains (as reviewed by Schroer, 2004; Levy and Holzbaur, 2006). $p150^{Glued}$ is crucial to dynactin complex because it binds directly to microtubules and improve the transport ability of dynein (King and Schroer, 2000). The first coiled-coil, or CC1 region is thought to bind directly to cytoplasmic dynein (King et al., 2003) and the second coiled-coil, or CC2

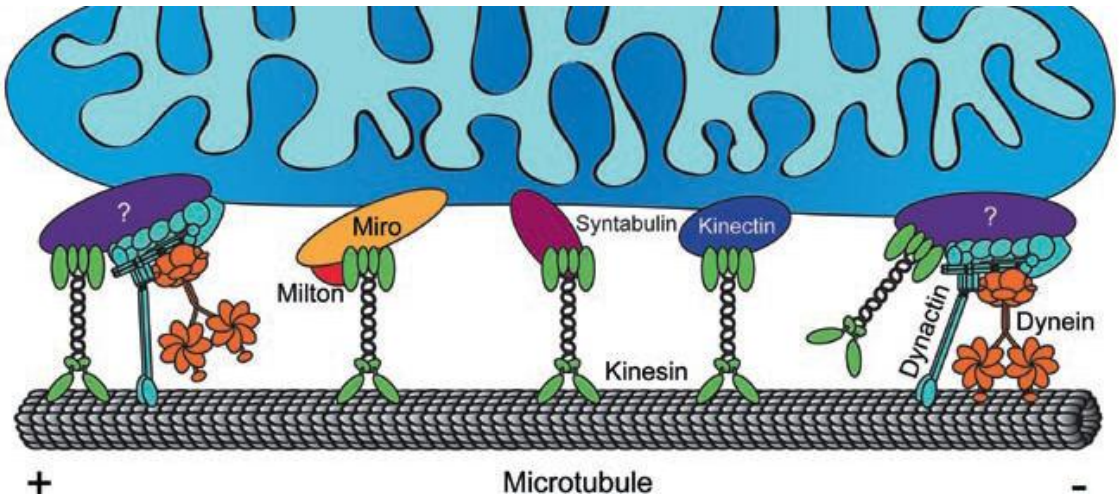

Figure 1.3: Mitochondria-associated motors and motor-cargo linker proteins.
Mitochondria, along with other cellular cargoes, require adaptor proteins to bind to motor proteins. One of the well-characterized adaptor protein complexes is the Miro/Milton complex that links mitochondria with KIF5. Syntabulin is another adaptor protein that has been implicated in binding mitochondria to kinesin. Kinectin is proposed to bind mitochondria to kinesin, however, the specific kinesin involved in the interaction remains unclear. An adaptor protein that links dynein/dynactin, which is responsible for retrograde movement, has yet to be determined. *(from Zinsmaier et al.2009)*.

region is believed to bind to the Arp1 rod (Waterman-Storer et al., 1995). The $p150^{Glued}$ protein has also been linked to kinesin-2, suggesting that dynactin may be involved in anterograde function (Berezuk and Schroer, 2007). The dynamitin subunit is another crucial component of the dynactin complex as it joins the $p150^{Glued}$ subunit and the Arp1 rod (as reviewed by Schroer, 2004). It consists of four dynamitin polypeptides that bind to each other through three coiled-coil regions (Echeverri et al., 1996; Schroer, 2004). Dynactin and dynein together control all of the 'minus'-end directed microtubule movement required for the cell; however, how the dynactin/dynein complex attaches to each specific cargo, such as mitochondria has yet to be determined.

1.1.1.5 Bidirectional Movement of Mitochondria and Other Organelles

Traditionally, the direction in which a cargo is being transported along axons was primarily determined by the nature of the motor driving its movement. It was previously

believed that, generally, if a cargo was bound to kinesin it would move anterogradely, or towards the periphery in axons and vice versa for a cargo bound to dynein/dynactin. However, recent studies have revealed a more complex model for axonal transport involving dynein and kinesin. These studies showed a co-dependence between kinesin and dynein and that the direction of a cargo's transport is determined by the coordination between the two and not which motor was bound, also known as bidirectional transport. In a study done by Deacon *et al.* (2003) dynactin was observed to bind dynein and kinesin-2 in *Xenopus laevis* melanophores. They specified that dynein and kinesin-2 were collectively joined by the $p150^{Glued}$ subunit of the dynactin complex. Colin *et al.*(2008) report that the huntingtin (htt) protein, which interacts with the intermediate chain of dynein, possesses the ability to determine a cargo's directionality. Using fluorescent brain-derived neurotrophic factor (BDNF) to observe vesicular transport, they found that a vesicle moved anterogradely when htt was phosphorylated and retrogradely when dephosphorylated (Colin et al., 2008) . Recent studies have also identified some of the cargoes that are involved in bidirectional transport. Mitochondria, for example, can exhibit bidirectional transport; they move in one direction, stop, and proceed in the opposite direction in the axon, where the polarity of microtubules is uniform and not mixed as in dendrites (as reviewed by Hollenbeck and Saxton, 2005). In light of recent studies, the transport of cargoes along the axon is not as simple as it once seemed. These observations point to a model where opposing motors can be bound to a cargo simultaneously and that its net movement is determined by a more complex mechanism than previously believed.

1.1.1.6 Possible Links Between Mitochondrial Trafficking Defects and Neuronal Injury

Most believe that the failure of mitochondria to meet metabolic and bioenergetic demands can lead to neuronal injury and cell death (as reviewed by Rintoul and Reynolds, 2009). Due to the high metabolic demand of distal regions of the neuron, defects in the transport and delivery of the mitochondria to these areas could contribute to cellular injury. One example is glutamate-mediated excitotoxcitiy. In

glutamate-mediated excitotoxicity, high concentrations of glutamate induce a massive influx of calcium into the cell primarily through NMDA receptors (Choi, 1988). A proportion of the incoming calcium is then buffered by mitochondria to the point where normal function is compromised (Stout et al., 1998). When this occurs, $\Delta\Psi m$ dissipates and ROS production increases, leading to cell death (Reynolds and Hastings, 1995; as reviewed by Mattson, 2003). In this model, as with other neurotoxin models, cell death is preceded by the disruption of mitochondrial movement, suggesting that mitochondrial trafficking may play a role in cell death via glutamate-mediated excitotoxicity.

In Huntington's disease, collections of polyglutamine forms of huntingtin, the protein that is thought as the cause of the disease, were associated with mitochondria (as reviewed by Chang et al., 2006; Rintoul and Reynolds, 2009). Defects in the motility of mitochondria in close proximity to these collections were also observed (Chang et al., 2006); however, deficiencies in the motility of other organelles were observed as well. Therefore, there is no direct link between the cessation of mitochondrial motility in these cells and ensuing cell death due the lack of specificity of these movement deficits of mitochondria. However, it is reasonable to hypothesize that mitochondrial trafficking and transport may play an important role in the progression or exacerbation of injury.

Another well-studied disease model is the amyotrophic lateral sclerosis model in mice. The main protein involved in this model is a mutant form of copper-zinc superoxide dismutase (mtSOD1) (Gurney et al., 1994). Previous studies by Kong and Xu (1998) showed a connection between motor neuron pathology and defects in mitochondrial morphology and distribution. Other studies show an association between mtSOD1 and mitochondria and a decrease in mitochondrial movement (De Vos et al., 2007). As to whether mtSOD1 is responsible for this defect in motility and trafficking has yet to be determined. Effects on mitochondrial distribution and function in the presence of mutant proteins, such as tau (Ebneth et al., 1998), amyloid precursor protein (APP) (Anandatheerthavarada et al., 2003), and apolipoprotein E4 (Chang et al., 2005) in Alzheimer's disease have also been documented (Mattson et al., 2008).

Despite these lines of evidence, it still remains unclear as to the contribution of mitochondrial trafficking defects to neuronal injury and cell death. As in the cases outline above, determining whether defective mitochondrial trafficking results in or is a product of neuronal injury and degeneration remains unanswered. In addition, in the cases of ALS and Huntington's disease all organelle transport was affected and not just mitochondrial. Clearly, the ability of mitochondria to provide energy to areas of high metabolic demand is essential to normal physiology and cell viability; however, it is unknown if cessation of movement alone is sufficient to begin a sequence of events that leads to death.

1.1.2 Mitochondrial Morphology

Many studies have established mitochondria as highly dynamic organelles not only in terms of movement and trafficking but in terms of morphology as well. Generally, mitochondria in neurons appear 'worm-like' and filamentous with sizes ranging from 1 to 2 microns to over ten microns. This shape, however, can change either by fusion or fission in response to different stimuli and is controlled by recently identified proteins (as reviewed by Chang and Reynolds, 2006; Liesa et al., 2009; Rintoul and Reynolds, 2009). The balance between the fission and fusion of mitochondria determine their morphology at any given moment within the cell. Why mitochondria fuse and divide in neurons and the impact of these processes on mitochondrial physiology remains unclear. However, some of the proteins that control this balance have recently been characterized. Proteins such as Dynamin-Related protein (Drp1) and Mitofusin-1 (Mfn1) and 2 (Mfn2) have received a great amount of attention for their functions in mitochondrial fission and fusion, respectively (as reviewed by Liesa et al., 2009; Rintoul and Reynolds, 2009).

1.1.2.1 Mitochondrial Fission

Mitochondrial fission was first observed as a process mediated by dynamin-related protein 1 (Drp1), a *C. elegans* gene (Labrousse et al., 1999). In mammals, the

protein dynamin 1-like protein/dynamin-related protein (DNM1L/DRP1) regulates mitochondrial fission (as reviewed by Liesa et al., 2009). Previous studies showed that overexpression of Drp1 lead to more punctate mitochondria not only in *C. elegans* but in neurons as well (Labrousse et al., 1999; Barsoum et al., 2006). In studies that inhibited the function of Drp1, mitochondria exhibited a more interconnected and elongated morphology (Smirnova et al., 1998). These results provide solid evidence to support the involvement of Drp1 in the control of mitochondrial fission. In addition, recent studies have examined possible mechanisms that modulate the action of Drp1, such as the possible link between mitochondrial fission and high calcium levels (Chang and Blackstone, 2007; Cribbs and Strack, 2007). In this suggested mechanism, the activation of calcineurin dephosphorylates Drp1 in response to high intracellular calcium levels, which then translocates to mitochondria and stimulates fission (Chang and Blackstone, 2007; Cribbs and Strack, 2007).

1.1.2.2 Mitochondrial Fusion

Mfn-1 and Mfn-2 are mammalian proteins that modulate mitochondrial fusion (as reviewed by Liesa et al., 2009; Rintoul and Reynolds, 2009). In the process of the fusion of two mitochondria (double membrane-bound organelles), two events occur; the fusion of the outer membrane and inner membrane. Since Mfn-1 and Mfn-2 are localized to the outer mitochondrial membrane, it is suggested that they are responsible for the initiation of the outer membrane fusion (Song et al., 2009). Studies that overexpressed mitofusins observed mitochondria as longer and more filamentous (Santel and Fuller, 2001). This provided evidence that Mfn-1 and Mfn-2 controlled mitochondrial fusion, however studies that employed mutant Drp1 in conjunction with overexpression of fusion proteins suggested that an equilibrium between the action of fission and fusion proteins determined the morphology of mitochondria (Santel and Fuller, 2001).

Optic Atrophy Protein 1 (OPA1) is another mammalian protein that is involved in mitochondrial fusion and is either bound to the inner mitochondrial membrane or

soluble in the intermembrane space (Alexander et al., 2000; Akepati et al., 2008). This suggests that OPA1 is involved in the initiation of inner mitochondrial membrane fusion (Song et al., 2009). Although the proposition that OPA1 initiates inner membrane fusion and the mitofusins control the outer membrane fusion seems logical, the exact sequence of events and action of these proteins in the mechanism of mitochondrial fusion has yet to be elucidated. In experiments where OPA1 was overexpressed, mitochondria were more fragmented, which contradicts its reported function as a fusion protein (Arnoult et al., 2005). This suggests that OPA1's involvement in fusion is complex and that this observation may be attributed to its many different isoforms and their alternative splicing (Delettre et al., 2001). The different isoforms may have the ability to interact with each other and are possibly dependent on other isoforms in order to regulate mitochondrial fusion (Song et al., 2007; Akepati et al., 2008). This could explain why different studies that used variants of the isoforms observed different effects on mitochondrial morphology. In addition to its involvement in mitochondrial fusion, OPA1 loss-of-function studies have reported activation of apoptosis due to its involvement in the maintenance of cristae morphology (Olichon et al., 2003). Through further investigation of OPA1 and its functions, it is clear that OPA1 not only regulates mitochondrial morphology, but it contributes to apoptosis as well. Its involvement and action in these processes appears very complex and requires further investigation.

1.1.2.3 Possible Links Between Mitochondrial Morphology and Neuronal Injury

There is very little information that documents any definite links between mitochondrial morphology and mitochondrial health and physiology. Many questions regarding the relationship between the shape of mitochondria and their bioenergetic and biochemical state remain unanswered. In addition, the question remains; does mitochondrial morphology have any contributions to neuronal injury and disease? Despite the correlations made between mitochondrial shape in some neurodegenerative diseases, there is no definitive evidence suggesting that imbalances in fission/fusion are the root cause of certain neurodegenerative diseases. However,

there is some evidence suggesting that changes mitochondrial morphology may play a part in neuronal injury and disease.

Some studies have investigated the connection between mitochondrial morphology and mitochondrial physiology and energetics. Many studies using mitofusins have reported an effect on mitochondrial metabolism. Bach et al. (2003) observed a reduction in glucose oxidation and oxygen consumption, which are involved in ATP synthesis when Mfn-2 was repressed. In another study, $\Delta\Psi m$ was decreased when Mfn-2 was repressed using antisense adenoviral expression (Pich et al., 2005). In addition to perturbations in mitochondrial fusion, disruptions in mitochondrial fission also produce similar decreases in $\Delta\Psi m$. Benard et al. (2007) observed reduced oxygen consumption and ATP synthesis in HeLa cells with DRP1 knockout using siRNA. These studies, along with many others, provide evidence suggesting a link between mitochondrial morphology and mitochondrial physiology and metabolism. It is apparent that disrupting the fission/fusion balance has an effect of mitochondrial physiology and metabolism, but does this defect lead to downstream events that eventually lead to cell death? Although mutations of certain morphology influencing proteins have been observed in some diseases, it has yet to be determined whether these diseases are a result of morphology defects or if these defects are a result of upstream events.

Mutations in mitochondrial morphology proteins have been investigated and characterized to a certain degree, however the precise contribution these mutations have in the pathway of neurodegeneration and disease have yet to be elucidated. In Charcot-Marie-Tooth Type 2A, which is characterized by chronic axonal degeneration of motor and sensory neurons, approximately twenty percent of cases are attributed to mutations in Mfn-2 (Lawson et al., 2005). Optic atrophy, a neurodegenerative disease characterized by the degeneration of retinal ganglion cells and subsequent atrophy of the optic nerve, is associated with mutations in OPA1 (Alexander et al., 2000). Despite the presence of the mutations that regulate mitochondrial morphology, it is clear that these mutations alone are not sufficient to cause cell death and that its contribution, along with additional insults, cumulatively compromises normal cell physiology, leading

to neuronal injury. Another notable fact is that even though these mutations are present in all cell types, only neurons exhibit any susceptibility to the mutations. From these observations, it is apparent that there is some unique characteristic of neuronal physiology that makes them more sensitive to defects in mitochondrial morphology regulation.

1.2 Rationale and Objectives

Previous studies have documented the disruption of mitochondrial movement following exposure to neurotoxins such as glutamate (Rintoul et al., 2003), nitric oxide (Rintoul et al., 2006; Zanelli et al., 2006), and zinc (Malaiyandi et al., 2005). Therefore, the main goal of this study is to investigate the direct consequences of mitochondrial motility disruption on mitochondrial dynamics and cell health and viability. This study may also provide some insight on the impact of mitochondrial transport disruption of cell health and its contribution to neurodegenerative diseases. The main hypothesis of this thesis is that disruption of mitochondrial motility, via CC1 overexpression, will have a significant impact on mitochondrial dynamics, physiology, and cell viability.

This study examined the effect of disrupting mitochondrial motility on mitochondrial morphology and physiology. The tool used to disrupt mitochondrial motility is overexpression of the first coiled-coil (CC1) region of the p150 ^{glued} subunit of dynactin. No previous studies have examined the effects of CC1 on mitochondrial dynamics and physiology; therefore, the following objectives were proposed.

Objective 1: Characterize the effects of CC1 overexpression on mitochondrial morphology, motility, and trafficking.

Objective 2: Characterize the effects of CC1 overexpression on mitochondrial physiology by assessing $\Delta\Psi m$ and calcium buffering.

Objective 3: Examine the impact of CC1 overexpression on cell viability and the cells' ability to recover from neurotoxin challenge.

2 MATERIALS AND METHODS

All chemicals were obtained from Sigma-Aldrich unless otherwise stated. In all experiments and during imaging a HEPES-buffered salt solution (HBSS) was used with the following composition (in mM): 137 NaCl, 5 KCl, 10 $NaHCO_3$, 20 HEPES, 5.5 Glucose, 0.6 KH_2PO_4, 1.4 $CaCl_2$, and 0.9 $MgSO_4$, adjusted to pH 7.4 using NaOH or HCl.

2.1 Cell Cultures

Primary dissociated neuronal cultures were obtained from embryonic Day 17 timed-pregnant Sprague-Dawley rats (provided by Charles River Canada and University of British Columbia). The dissection was performed with cold, sterile dissection HBSS (dHBSS) (5.365mM KCl, 0.441mM KH_2PO_4, 0.137mM NaCl, 0.634mM Na_2HPO_4-$7H_2O$, and 10mM HEPES) in a dish on ice under a Leica SMZ645 Dissecting microscope. Brains from the embryos were removed and placed in separate dish with cold dHBSS on ice. Cortices from each embryonic brain were then isolated and placed into a 35mm dish with cold dHBSS on ice. Then isolated cortices placed in a dish with 4mL dHBSS + 600µL Trypsin-EDTA (0.25%) (Invitrogen) and incubated at 37^{o}C for 30 minutes.

After incubation, the cell suspension was placed into a polypropylene centrifuge tube and gently triturated until uniform. Cold neurobasal (NB) (Invitrogen) media supplemented with B27 with antioxidants (NB+AO) (Invitrogen) was added and further triturated to mix the solutions and subsequently passed through a 70µm cell mesh (VWR) into a new tube. The tube was centrifuged at 1300rpm (340 X g), at 20^{o}C for 3 minutes or until a pellet was formed. The supernatant was decanted and the pellet was resuspended in NB+AO and centrifuged again using the same conditions. After discarding the supernatant, the washed pellet was resuspended in fresh NB+AO media.

The cell concentration of this suspension was determined using a haemocytometer (Hausser Scientific) and cell viability assessed using Trypan Blue. If cell viability was below 85% the cells were not plated. If the suspension was suitable for plating, it was diluted to obtain a final concentration of 700, 000 cells per mL. 1mL of the cell suspension was placed in each well of a 12-well culture dish (Corning) containing one 18mm glass coverslip (VWR) coated with poly-D-Lysine. The plates were then incubated in a humidified atmosphere of 5% CO_2/95% Air at 37°C.

After four days *in vitro* (DIV) the media was changed with the follow protocol: the plating media was removed and coverslips were rinsed briefly with 500µL of warm, unsupplemented NB media before replacement with 1mL of NB supplemented with B27 without antioxidants (NB-AO). Cells were subsequently fed on DIV 8, 11 and 14 by removing 250µL of media in each well and replacing it with 300µL of fresh NB-AO. The media removed from each different feeding (conditioned media) was filter-sterilized and kept at 20^{o}C for later use in the transfection protocol.

The astrocytes used in all experiments were D1 post-partum primary rat cortical astrocytes generously provided by Dr. Michael Silverman.

2.2 DNA constructs and Transfections

To visualize mitochondria within the cell, a mitochondrially-targeted enhanced yellow fluorescent protein (mt-eYFP) construct was used (courtesy of Dr. Roger Y. Tsien, University of California, San Diego). It consists of the eYFP gene and the targeting sequence from subunit IV of cytochrome C oxidase, which targets the eYFP gene to mitochondrial matrix, inserted into the pCDNA3 vector (Invitrogen), a mammalian expression vector(Llopis et al., 1998). The CC1-CFP was originally given to us as CC1-green fluorescent protein (GFP) by Dr. Kevin Pfister, University of Virginia. However, since YFP was used to label the mitochondria, GFP was replaced with CFP in the CC1 fusion construct. The empty vector expressing cytosolic CFP was transfected along with mt-eYFP in the control group. The Neuropeptide-Y (NPY) cherry plasmid was generously

provided by Dr. Michael Silverman. All plasmids and constructs were amplified and reproduced using the Qiagen Maxi-prep kits according to the protocol provided by the manufacturer.

Transfections were performed on primary cortical neurons at DIV 13-15 and astrocytes using Lipofectamine 2000 (LF 2000) (Invitrogen). The following amounts of each DNA plasmid were used in the transfection protocol: 0.75µg of mt-eYFP, NPY-cherry, and cyto-CFP and 0.5µg of CC1-CFP per coverslip. In the transfection protocol the ratio of LF 2000 to amount of DNA was 1.5µL of LF 2000 for every 1µg of DNA in the reaction. The transfection reagents were placed in each well and incubated for 12-16 hours. The media of the transfected wells were removed and replaced with conditioned media; media that was removed during the DIV 8, 11, and 14 feeding of the neurons. Transfected coverslips were imaged 24-36 hours after the media change. The LF 2000 protocol regularly yielded a transfection efficiency of 1-2%, allowing us to image approximately one neuron per field using a 40X objective.

2.3 Fluorescent Imaging

In all experiments, cells were visualized using a Nikon TE-2000-E epifluorescent microscope equipped with a Lambda-LS Xenon Arc lamp (Sutter) controlled by SimplePCI Imaging software (Compix, Inc.). Cells were imaged using a 40X (Extra-long working distance) objective and digital cooled CCD camera (Orca-ER Hamamatsu). Fluorescent exposure times were adjusted to obtain a high fluorescence intensity and minimal signal saturation.

2.4 Data Acquisition and Analysis

2.3.1 Mitochondrial Morphology and Distribution

Mitochondrial morphology was assessed using still images of YFP-labelled mitochondria in primary cortical neurons and astrocytes. Using SimplePCI, individual

mitochondria were traced and mean length in µm was measured. For primary cortical neurons, mean percent filling of mitochondria and mean number of mitochondria per µm were measured to assess mitochondrial distribution or trafficking. To obtain mean percent filling of mitochondria in a neuronal process the total length of the mitochondria within the process was added and divided by the total length of the neuronal process. For mean number of mitochondria per µm we divided the total number of individual mitochondria measured by the total length of the neuronal processes to normalize for the varying lengths of processes measured. To assess mitochondrial distribution in astrocytes, SimplePCI was used to measure the total area of the cell (using CFP images which outline cellular boundaries since cyto-eCFP and CC1-CFP were cytoplasmic) and the total area that was occupied by mitochondria. The mitochondrial area was then divided by the total cellular area to obtain a mean percent filling by mitochondria.

2.3.2 Mitochondrial and Organelle Movement

For mitochondrial movement experiments time lapse image sequences of YFP-labelled mitochondria or any other fluorescently labelled organelle were obtained at a rate of 6 images per minute or 1 image every 10 seconds for 2 minutes at 37^{o}C. Then a random 255 x 255 pixel region of the cell was cropped and used for analysis. Mitochondrial movement was measured as previously described (Rintoul and Baimbridge, 2003). Briefly, successive images are subtracted and increases or decreases in intensities over the threshold or “movement events” between the two images are added and the total movement events for a sequence are determined. The total number of events for a sequence was then divided by the total number of pixels occupied by mitochondria to normalize for the different number of mitochondria between cells. The final parameter obtained and used for comparison was mean events/pixel.

In primary cortical neurons, the cropped 255 x 255 regions were used in further mitochondrial anterograde/retrograde trafficking analysis. In these experiments the total number of mitochondria moving anterogradely or retrogradely for a distance

greater than 2µm were added and normalized by dividing by the total length of the process to obtain the mean number of anterograde/retrograde moving mitochondria per µm. The mean number of mitochondria exhibiting vectorial movement per µm was also attained by adding the number of mitochondria moving retrogradely and anterogradely and normalizing with the total process length.

2.3.3 Calcium Dynamics

To monitor intracellular calcium levels we used Mag-Fura 2 (Invitrogen), a low affinity calcium indicator. Prior to imaging, transfected coverslips were loaded with 5µM of Mag-Fura 2 in HBSS + 0.5% bovine serum albumin (BSA) (Fisher Scientific) at 37^{o}C for 15 minutes. Coverslips were then washed with HBSS twice and imaged. When observing Mag-Fura 2 levels within the cell, intracellular calcium levels ($[Ca^{+2}]_i$) were reported as a ratio between emitted fluorescence intensities at 340nm and 380nm excitation and were proportional to $[Ca^{+2}]_i$ (a high ratio indicates high $[Ca^{+2}]_i$ and vice versa).

To manipulate $[Ca^{+2}]_i$ we used glutamate to induce an influx of extracellular calcium into the cell and subsequently mitochondria. Following glutamate treatment Carbonylcyanide-p-(trifluoromethoxy)-phnylhydrazone (FCCP) was employed to depolarize the mitochondria and release calcium sequestered in mitochondria into the cytoplasm. The time course of the Mag-fura 2 experiment went as follows: 7 minutes of perfusion with HBSS alone, 5 minutes 30µM glutamate/1µM glycine in HBSS, 10 minutes with HBSS alone, and 5 minutes with 750nM FCCP in HBSS with images captured every 20 or 40 seconds. Background subtracted 340/380 ratios were recorded and the following parameters that indicate a cells ability to manage influxes of calcium were determined: change in Mag-Fura 2 ratio during glutamate stimulation, area-under-the-curve (AUC) during glutamate stimulation, change in Mag-Fura 2 ratio during FCCP stimulation, AUC during FCCP stimulation, and the FCCP AUC/glutamate AUC ratio.

2.3.4 Mitochondrial Membrane Potential

In experiments looking at ΔΨm, tetramethylrhodamine methyl ester (TMRM) (Cedarlane) was used. Right before transfected cells were imaged, coverslips were loaded with 200nM of TMRM at 37^{o}C for 30 minutes. After incubation, coverslips were washed with HBSS twice and then imaged. Coverslips were exposed to the following treatment: perfusion with HBSS + 20nM TMRM for 7 minutes then perfusion with 750nM FCCP in HBSS for 5 minutes. $\Delta F/F_o$ was calculated and used form comparison. ΔF was obtained by subtracting the mean baseline intensity (F_o) from the highest observed fluorescence intensity (F_f) during FCCP stimulation. ΔF was then divided by F_o to normalize for the differing baseline values.

2.3.5 Cell Survival

Cells were assessed on their ability to survive a glutamate challenge to determine the global cellular effect of mitochondrial transport disruption. In these experiments, control and CC1-transfected cells were exposed to three different conditions 24hrs prior to imaging: negative control (HBSS alone), positive control (excessive exposure to glutamate), and the experimental treatment (30μM glutamate/1μM Glycine). For the positive controls, cells were treated with 250μM glutamate + 1μM glycine overnight to ensure cell death. In the experimental treatment, cells were given a glutamate challenge with 30μM glutamate + 1μM glycine for 10 minutes at 37^{o}C. The glutamate/glycine solution was removed and replaced with the original media. For the negative controls, cells were washed with HBSS alone. We calculated two parameters from these experiments: percent viability and survival. Viability rate determined the impact of CC1 on the general health of the cell and survival rate assessed the effect of CC1 on a cell's ability to recover from a glutamate challenge. To obtain viability rate the total number of CFP-positive cells (cells that were previously confirmed as viable cells with Hoechst staining) present in the negative controls for each treatment were counted in three adjacent rectangular areas that span the vertical diameter of the coverslip. To calculate survival rate, the total number of live cells

present in the same three regions of an experimental treatment coverslip were counted and then divided by the number of live cells counted in the negative controls. This gave us a percentage of cells that survived (% survival) the glutamate challenge.

2.3.6 Statistical Analysis

Comparisons of all measured parameters between the two groups were achieved using the Student's unpaired *t*-test. When determining if a difference is significant a *p*-value of 0.05 was used. All values are report as means ± standard error of the mean (S.E.M).

3 RESULTS

In all experiments of this project, mt-eYFP was used to label the mitochondria within primary cortical neurons and astrocytes. The controls were co-transfected with cytoplasmic CFP and the cells in the treatment group were co-transfected with CC1-CFP, which disrupts the dynein/dynactin complex. The CC1-CFP construct codes for the first coiled-coil region of the $p150^{Glued}$ subunit in the dynactin complex. It is responsible for binding to cytoplasmic dynein and recruiting it to the dynactin complex, where its functions can be carried out. Therefore, overexpression of the CC1 construct will bind to the free cytoplasmic dynein and prevent it from binding to the endogenous p150 subunit, and subsequently disrupt the function of the dynein motor (Quintyne et al., 1999). The LF 2000 protocol was used to regularly obtain a transfection efficiency of approximately 1%, allowing us to visualize approximately one cell within any given field. Images were then captured and subsequently analyzed according to the protocol outlined for the particular experiment.

3.1 Mitochondrial Morphology

No previous studies have examined the effect of CC1 on mitochondrial dynamics; therefore, the first step was to observe the effect of CC1 on the morphological dynamics of mitochondria. Mitochondrial morphology was compared between controls and cells that have disrupted mitochondrial movement. In control astrocytes transfected with mt-eYFP, the mitochondria have an elongated morphology; however, astrocytes transfected with CC1 show a dramatic change in morphology. The mitochondria in the CC1-transfected cells appear smaller and more punctate (figure 3.1). To quantify these observations, mitochondrial length was measured and compared between controls and

CC1-transfected astrocytes. The mean mitochondrial length in the controls (2.78 ± 0.12 µm, N=10 cells) was significantly longer than the CC1-transfected cells (2.18 ± 0.11 µm, N=10 cells; $p<0.05$; t-test) (figure 3.2). This morphological effect was also observed in primary cortical neurons (figure 3.3). Neuronal mitochondria within the treatment group exhibited a very similar morphology to the mitochondria of astrocytes treated with CC1, where the mitochondria were small and punctate compared to the controls. Mean mitochondrial length of the controls (3.199 µm ± 0.088, N=10 cells) was significantly longer than that of the CC1-transfected neurons (2.138 µm ± 0.056, N=10 cells; $p<0.05$; t-test) (figure 3.4). These results suggest that disrupting mitochondrial movement has an effect on the morphology of mitochondria within astrocytes and cortical neurons causing a significant decrease in length.

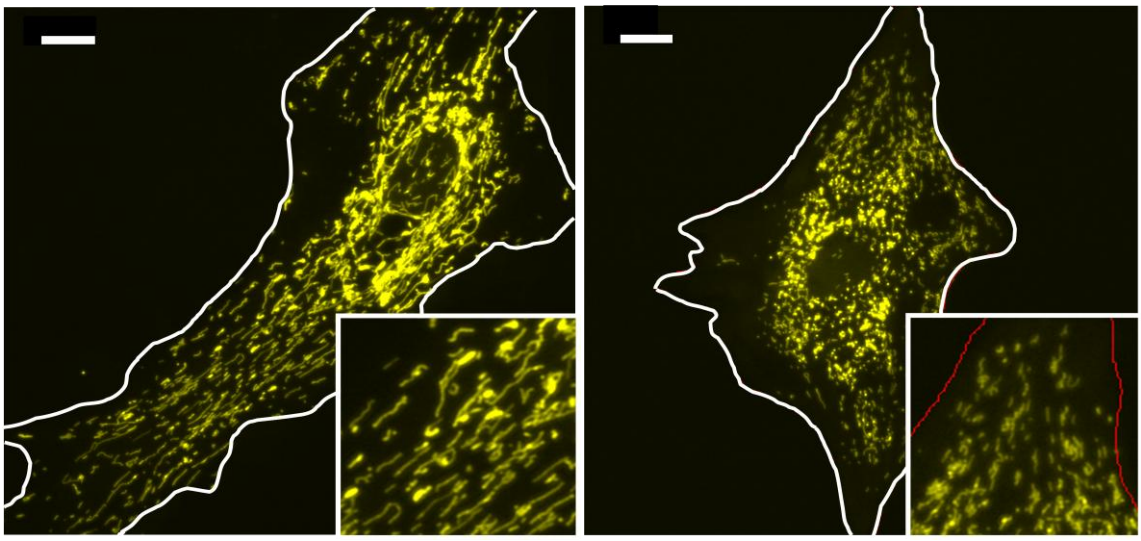

Figure 3.1: CC1 has a significant effect on mitochondrial morphology and distribution in cortical astrocytes.
Cortical astrocytes transfected with mt-eYFP and cytosolic-CFP (control) or CC1-CFP at 40X objective. The white line denotes the cellular boundary and inset images show magnified mitochondria. (A) Control astrocyte has long mitochondria that are dispersed around the cell, while (B) a CC1 transfected astrocyte exhibits round, punctate mitochondria that cluster near the nucleus. White bar denotes a scale of 30µm.

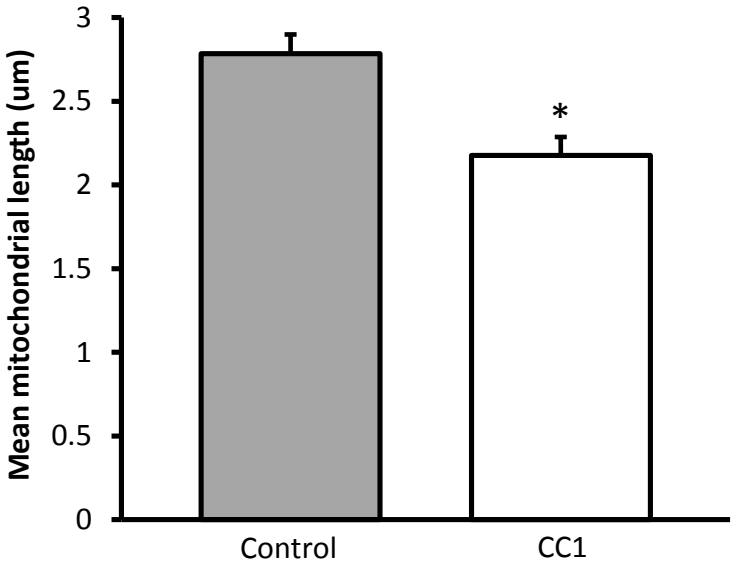

Figure 3.2: CC1 significantly decreased mitochondrial length in cortical astrocytes.
Mean mitochondrial length was measured in control and CC1-transfected cortical astrocytes. Mitochondria in the CC1 cells were significantly shorter than that of the control cells ($p<0.05$ using student's t-test; control, n=10 cells; CC1, n=10 cells). * denotes a significant difference from the control. Values expressed as means ± S.E.M. in µm.

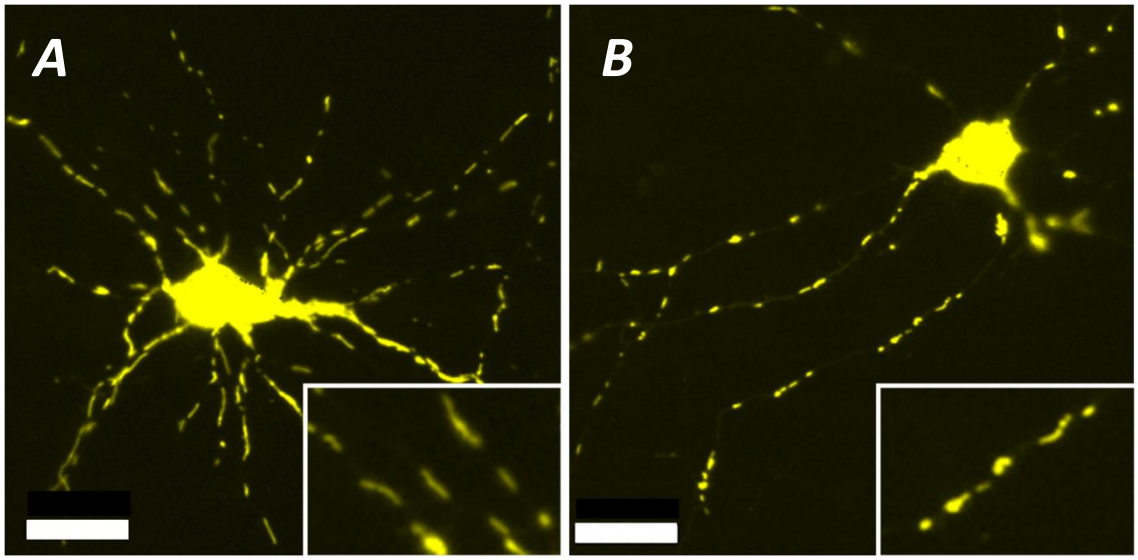

Figure 3.3: CC1 has a significant effect on mitochondrial morphology in primary cortical neurons.
Primary cortical neurons transfected with mt-eYFP and cytosolic-CFP (A) or CC1-CFP (B) at 40X magnification. Inset images are magnified images of mitochondria within a neuronal process. (A) A control neuron showing long mitochondria and a CC1 neuron (B) showing a significant change to smaller, punctate mitochondria. White bars denote a scale of 20µm.

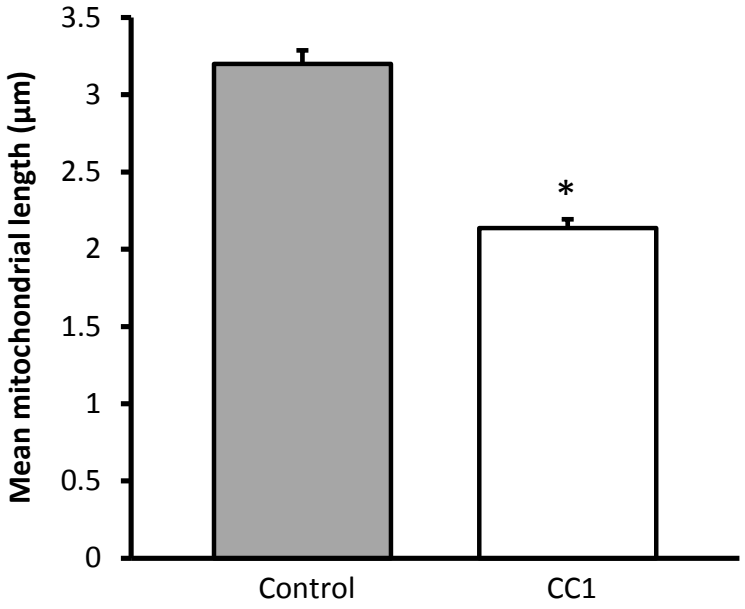

Figure 3.4: CC1 significantly decreased mitochondrial length in primary cortical neurons. Mean mitochondrial length was measured in control and CC1 primary cortical neurons. Mitochondria of CC1 cells were significantly shorter than mitochondria of control cells ($p<0.05$ using student's t-test; control, n=10 cells; CC1, n=10 cells). * denotes a significant difference from controls. Values expressed as means ± S.E.M. in µm.

3.2 Mitochondrial Motility and Trafficking

3.2.1 Mitochondrial motility

We next examined the effect of CC1 on the movement and trafficking of mitochondria in astrocytes and neurons. Time lapse image sequences of the YFP-labelled mitochondria were obtained from the control and treatment groups at a rate of one image every 10 seconds for a total of 2 minutes. These sequences were then analyzed as described in Rintoul et al. (2003). Briefly, changes in fluorescence intensities, both light-to-dark decreases and dark-to-light increases over a threshold of ten intensity units between two adjacent images in a sequence are detected. Each detected change in pixel intensity is considered a movement event and the movement events between each adjacent field are then added up and normalized to obtain the mean movement events per pixel. The number of movement events is divided by the

number of total pixels above the defined threshold to normalize for the varying number of bright objects (mitochondria) present within the field. This method provides an estimation of the bulk mitochondrial movement of a cell; however, it does not provide more detailed movement parameters such as velocity or run length. It quantifies all types of movement from long range vectorial movement to small lateral movements or 'wiggling' of mitochondria.

Mitochondrial movement in astrocytes was significantly affected in cells transfected with CC1. In control astrocytes, the mean movement events per pixel was 0.21959 ± 0.02034 (N=13 cells); however, the mean movement events per pixel in CC1-transfected cells was significantly decreased to 0.15574 ± 0.01556 (N=16 cells; $p<0.05$; t-test) (figure 3.5). A similar decrease in movement was observed in cortical neurons transfected with CC1. The mean movement events per pixel in the controls was 0.26016 ± 0.01707 (N=14 cells) and the mean movement events per pixel in CC1-transfected cells was significantly lower than the controls at 0.12445 ± 0.00983 (N=29 cells; $p<0.05$; t-test) (figure 3.6).

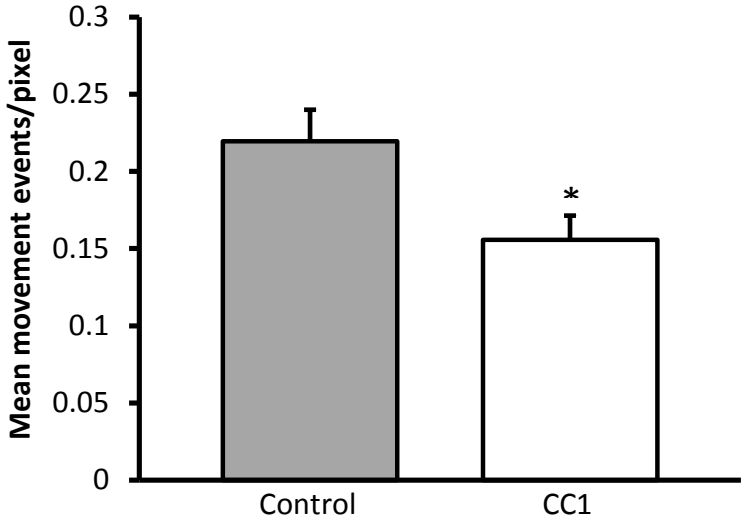

Figure 3.5: CC1 significantly decreased mitochondrial movement in cortical astrocytes. Mean mitochondrial movement, expressed as movement events/pixel was measured as previous described (Rintoul et al., 2003) in control and CC1 cells. Mitochondrial movement was significantly reduced in CC1 cells when compared to controls ($p<0.05$ using student's t-test; control, n=13 cells; CC1, n=16 cells). * denotes a significant difference from controls. Values expressed as means ± S.E.M.

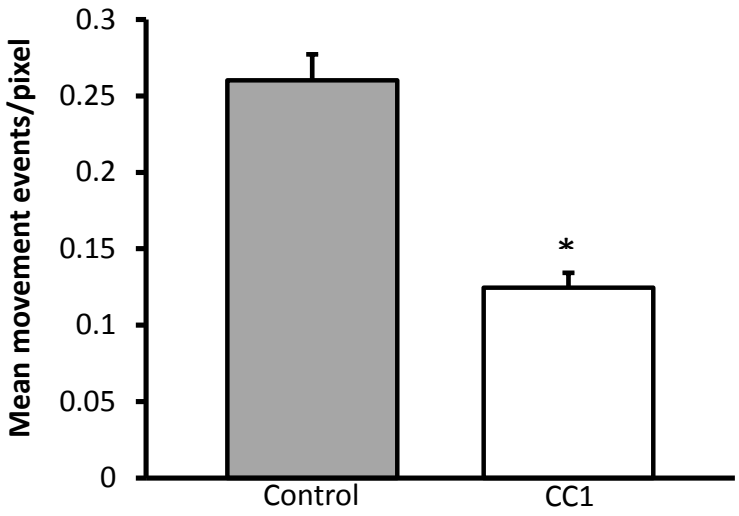

Figure 3.6: CC1 significantly decreased mitochondrial movement in cortical neurons. Mitochondrial movement, expressed as movement events/pixel was measured in control and CC1 cells. Mitochondrial in controls were significantly more mobile than those in CC1 cells ($p<0.05$ using student's t-test; control, n=14 cells; CC1, n=29 cells). * denotes a significant difference from controls. Values expressed as means ± S.E.M.

3.2.2 Mitochondrial Trafficking

With the decrease in mitochondrial movement observed in CC1 transfected cells, the effect of CC1 on mitochondrial trafficking was then examined. In this experiment, the distribution of the mitochondria in neuronal processes was investigated to assess whether there was a change in mitochondrial trafficking. To answer this question, single images of mitochondria were examined in the controls and the CC1 transfected cells. For the astrocytes, the area of the cell was measured by analyzing the CFP images in both controls and CC1 cells and the area occupied by the mitochondria. We then divided the cell area by the area occupied by the mitochondria to establish the portion of the cell that is occupied by the mitochondria. This provided us with a quantitative measure of changes in mitochondrial distribution.

In astrocytes, the mitochondria of the CC1 transfected cells are more abundant and concentrated around the nucleus of the cell; the controls however, appear to have mitochondria that are fairly diffuse and dispersed around the entire cellular volume

(figure 3.1). The quantitative analysis of mitochondrial distribution supports this observation showing a decrease in the percentage of total cell area occupied by the mitochondria in cells transfected with CC1 (figure 3.7). In these cells the area occupied by mitochondria (0.3623 ± 0.0311% ,N=9 cells) was significantly lower compared to controls (0.4989 ± 0.0526%, N=9 cells; $p<0.05$; t-test).

To see if this effect occurred in neurons, we analyzed still images of mitochondria in a process of a neuron, which were mostly dendrites. Within this process we traced all the discrete mitochondria that were present. We also measured the total length of the process. With these parameters we determined the mean number of mitochondria per µm and the percent filling of mitochondria within the process (total mitochondrial length/total process length). The number of individual mitochondria per µm of neuronal process was surprisingly unaffected (figure 3.8). The mean number of

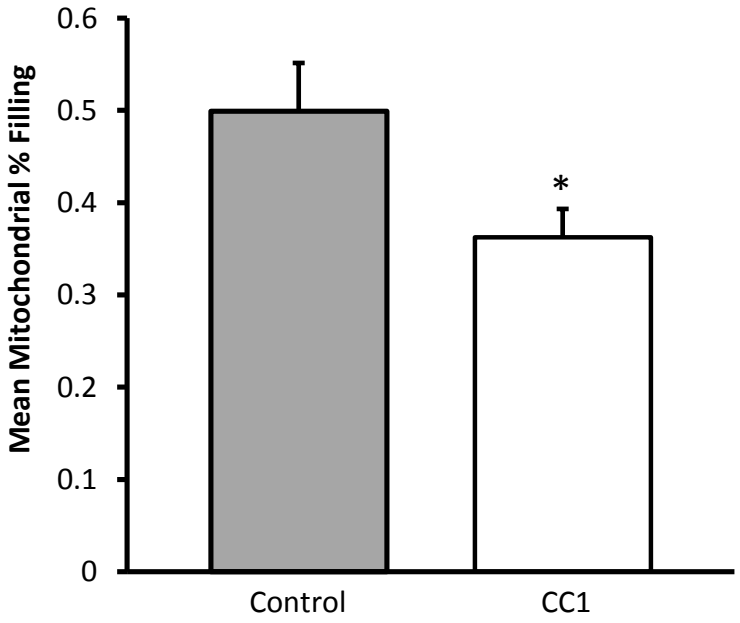

Figure 3.7: CC1 significantly decreased the area occupied by mitochondria in cortical astrocytes.
Mean mitochondrial distribution, expressed as percent filling was measured in controls and CC1 cells. Mitochondria of the controls occupy a significantly larger cellular area than mitochondria within CC1 cells ($p<0.05$ using student's t-test; control, n=9 cells; CC1, n=9 cells). * denotes a significant difference from controls. Values expressed as mean ± S.E.M.

mitochondria present per µm was 0.0724 ± 0.0051 (N=21 cells) for the controls and 0.0636 ± 0.0029 (N=38 cells; p=0.14; t-test) for the CC1 cells. The percent filling of mitochondria, however, was significantly reduced in the CC1 cells (figure 3.9). The mitochondria in CC1 transfected cells filled 25.82 ± 2.97% (n=10 cells) of the process while the mitochondria of the controls filled approximately double the length of the process at 58.78 ± 5.09% (n=10 cells; $p<0.05$; t-test). Using the still image analysis, the distribution of mitochondria appears to be differentially affected by CC1 when comparing astrocytes and neurons. In astrocytes, the majority of mitochondria were located close to the nucleus; however, neuronal mitochondrial distribution appeared to be unaffected.

Further analysis of CC1 and controls cells was performed to assess the trafficking of mitochondria within cortical neurons. More specifically, the amount anterograde and retrograde movement of mitochondria was measured. To compare the two groups, the image sequences used to obtain mean events per pixel (movement analysis) were analyzed for the number of mitochondria moving in an anterograde and retrograde direction. In each sequence, one random process was chosen for the analysis, and in each process, the number of mitochondria that exhibited vectorial movement, which is defined as movement towards the cell body (retrograde) or cell periphery (anterograde) for a distance greater than 2µm were counted. The number of moving mitochondria was then divided by the total length of the process to normalize for the varying lengths of processes between cells and the mean number of mitochondria moving in a retrograde and anterograde direction per µm was determined. The total number of moving mitochondria was also calculated by adding the number of anterograde and retrograde moving mitochondria and normalized by dividing this total by the total length of the process.

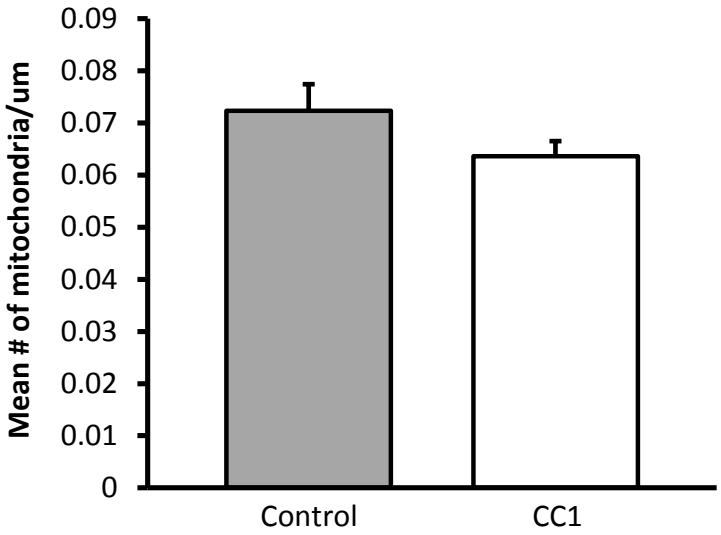

Figure 3.8: CC1 had no effect on the number of mitochondria in a neuronal process.
Mean number of mitochondria in a neuronal process per µm was determined in controls and CC1 cells. There was no significant difference in number of mitochondria per µm in controls and CC1 cells (p=0.14 using student's t-test; control, n=21 cells; CC1, n=38 cells). Values expressed as means ± S.E.M.

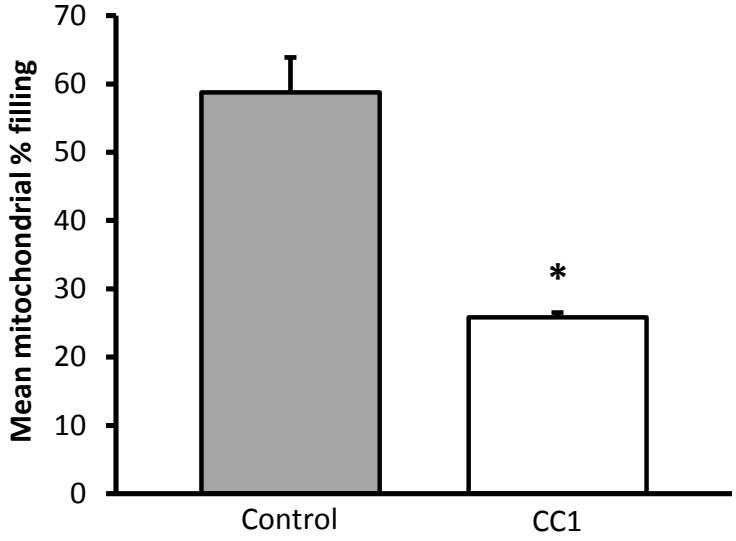

Figure 3.9: CC1 significantly decreased the area occupied by mitochondrial along a neuronal process.
Mean mitochondrial percent filling was measured in controls and CC1 cells. Mitochondria within the controls filled a significantly larger portion of the process when compared to the CC1 cells. Values expressed as means ± S.E.M. ($p<0.05$ using student's t-test; control, n=10 cells; CC1, n=10 cells). * denotes a significant difference from controls. Values expressed as means ± S.E.M.

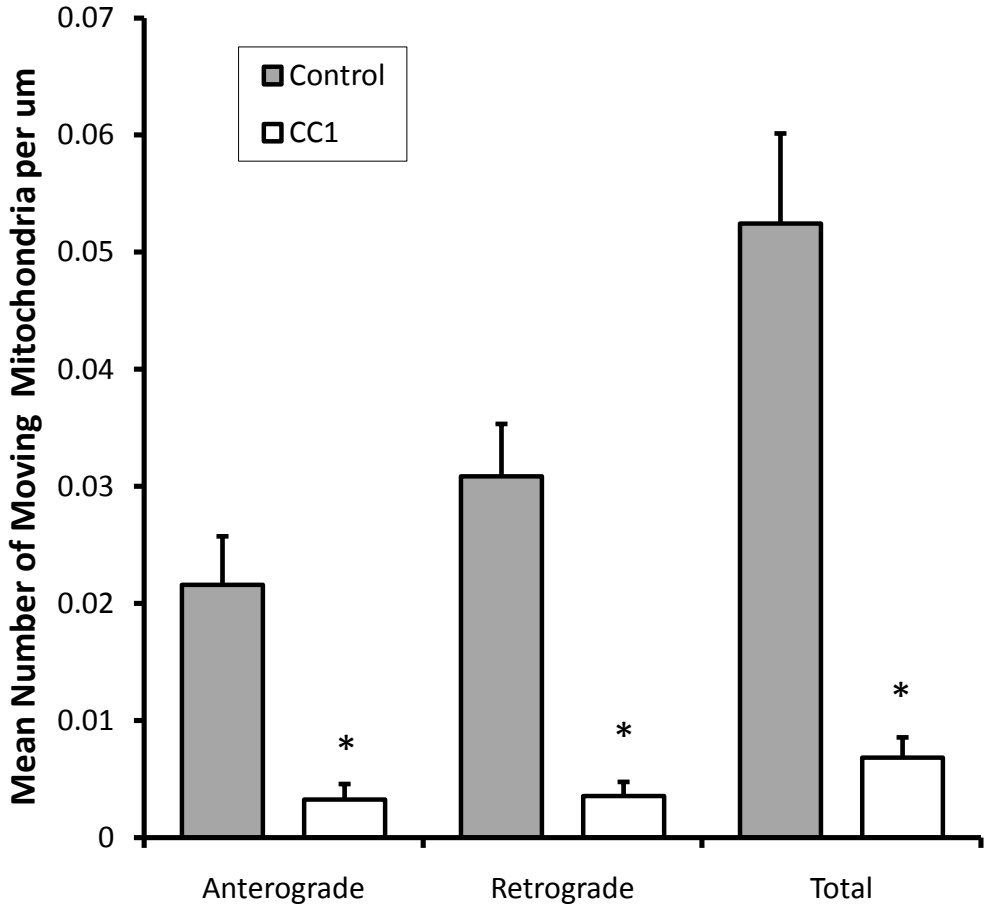

Figure 3.10: CC1 significantly decreased the trafficking of mitochondria within a neuronal process.

Mean number of mitochondria moving either retrogradely or anterogradely for a distance greater than 2µm was determined in controls and CC1 primary neurons and expressed as number of moving mitochondria per µm of neuronal process. Total number of moving mitochondria was calculated by adding the number of anterograde and retrograde moving mitochondria. In the case of CC1 cells, mitochondria moving in the anterograde and retrograde direction were significantly reduced when compared to controls ($p<0.05$ using student's t-test; control, n=26 cells; CC1, n=49 cells). * denotes a significant difference from controls. Values expressed as means ± S.E.M.

CC1, as predicted, had an effect on mitochondrial movement. However, CC1 had a significant effect on not only retrograde movement but anterograde movement as well. In examining retrograde movement the mean number of mitochondria moving per µm decreased approximately ten-fold from 0.0309 ± 0.0045 (N=26 cells) in the controls to 0.0036 ± 0.0012 (N=49 cells; $p<0.05$; t-test) in CC1. The same effect was seen in the mitochondria moving in the anterograde direction. For anterograde mitochondria, the mean also decreased nearly ten-fold as well from 0.0216 ± 0.0042 (N=26 cells) in the controls to 0.0033 ± 0.0013 (N=49 cells; $p<0.05$; t-test) in CC1. The total vectorial movement of mitochondria in neurons significantly decreased from 0.0525 ± 0.0077 (N=26 cells) in the controls to 0.0068 ± 0.0017 (N=49 cells; $p<0.05$; t-test) in CC1. From these results it is apparent that CC1 has a significant effect on the trafficking of mitochondria, significantly reducing the trafficked mitochondria in both the retrograde and anterograde direction.

3.2.3 Motility of Other Organelles

After observing the effects of CC1 on mitochondria motility it was examined whether this significant decrease in movement was specific to mitochondria. To investigate this, controls and the CC1 cells were co-transfected with NPY-cherry, a construct that identifies dense core vesicles (Kwinter et al., 2009). Cells were then imaged and sequences of images of NPY vesicles were obtained and analyzed with the same procedure used in the mitochondrial movement analysis. From the analysis, it was apparent that CC1 significantly decreased the movement of NPY vesicles. The mean movement events per pixel was 0.210 ± 0.018 (N=9 cells), approximately half the mean of the controls (0.436 ± 0.064, N=17 cells; $p<0.05$; t-test). Clearly, CC1 not only decreases the movement of mitochondria but it also affects the movement of other organelles as well.

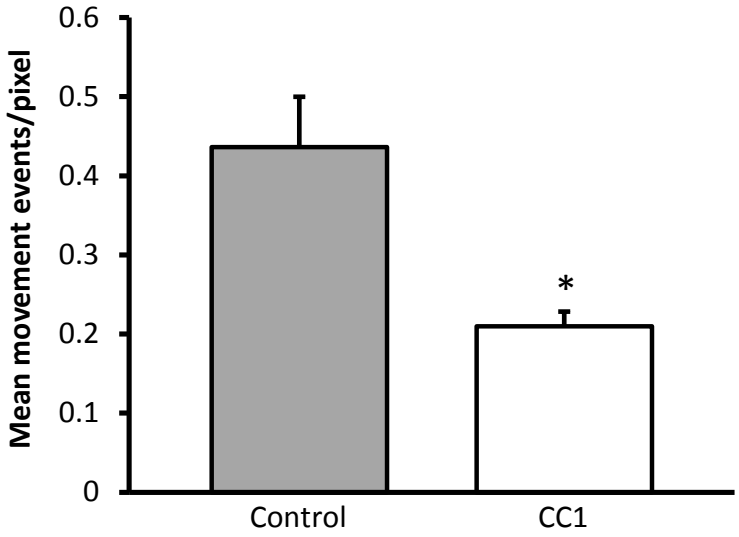

Figure 3.11: CC1 significantly decreased the movement of NPY vesicles in cortical neurons. Movement of NPY vesicles, expressed as movement events per pixel, was measured in control and CC1 primary cortical neurons. Movement of these vesicles was significantly reduced in CC1 transfected neurons compared to controls ($p<0.05$ using student's t-test; control, n=17 cells; CC1, n=9 cells). * denotes a significant difference from controls. Values expressed as means ± S.E.M.

3.3 Mitochondrial Calcium Dynamics

It is widely accepted that one of the major physiological functions of mitochondria is to buffer intracellular calcium (as reviewed by Duchen, 2004). Mitochondria, along with the endoplasmic reticulum are employed by the cell to modulate the calcium levels intracellularly. When large influxes of calcium are not controlled harmful downstream effects occur, which may lead to excitotoxic cell death as described above (Olney and de Gubareff, 1978). The experiments described in this section examine the changes in mitochondrial physiology in response to disruption of their transport. To monitor intracellular calcium levels, we used Mag-Fura 2; a low-affinity calcium indicator that reports intracellular calcium levels as a ratio of fluorescence emission intensity detected at 340 and 380 nm excitation. Brocard *et al.* (2001) demonstrated that glutamate stimulation, primarily through NMDA receptor activation, triggers an influx of extracellular calcium into the cell and that a portion of the incoming

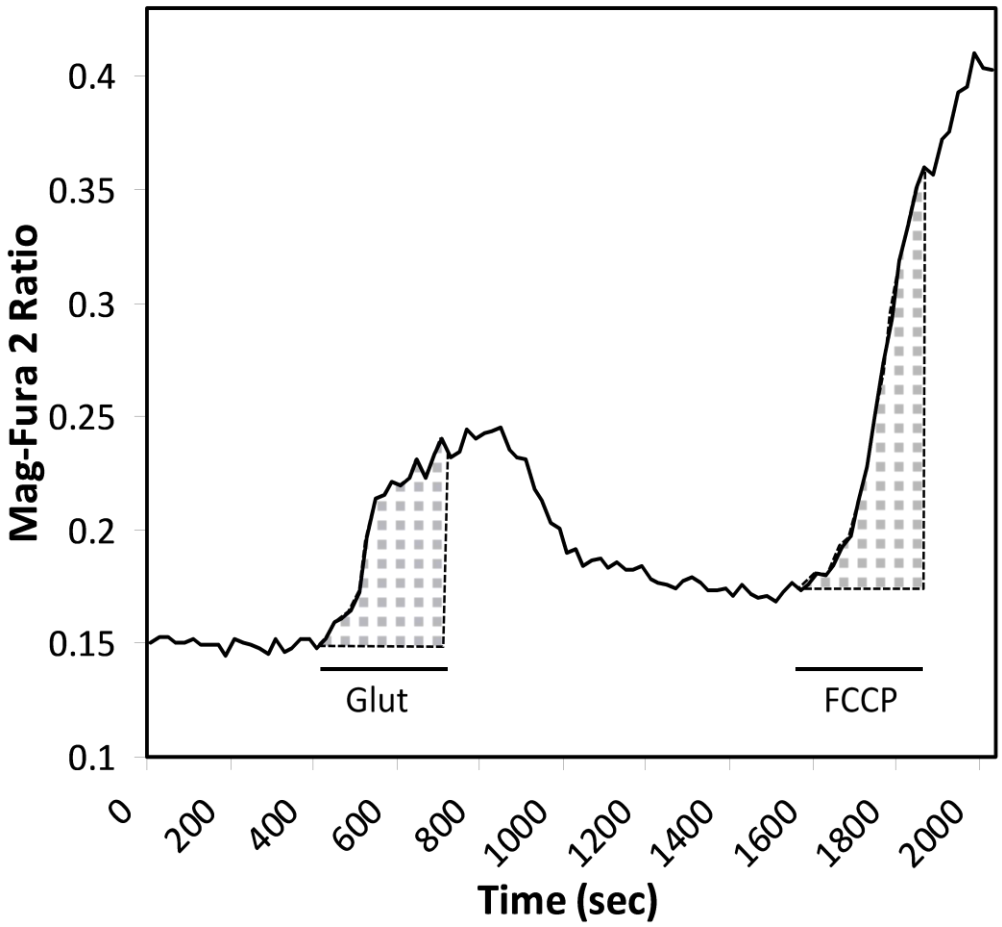

Figure 3.12: Measuring calcium dynamics in cortical neurons employing Mag-fura 2.
A representative trace of Mag-Fura 2 ratios over the course of a glutamate challenge to assess mitochondrial calcium buffering ability in cortical neurons. Cells in both groups that were included in the analysis exhibited a similar trend: stable baseline; increase in mag-fura 2 ratios during glutamate stiumulus; decrease in mag-fura 2 ratios during recovery; and finally an increase in mag-fura 2 ratios during FCCP stimulation. Cells that did not recover from or react to the glutamate stimulus were not included in the analysis. From this trace the following parameters were obtained: peak Ca^{+2} during glutamate stimulation; peak Ca^{+2} during FCCP stimulation; Peak FCCP/Glut Ca ratio; glutamate AUC (glutamate dotted area); FCCP AUC (FCCP dotted area); and FCCP/Glut AUC ratio.

calcium is buffered by mitochondria. With this in mind, we used glutamate to induce an influx of calcium into the cell and subsequent uptake of that calcium into the mitochondria. We then exposed the cells to FCCP, a protonophore that rapidly dissipates the ΔΨm, releasing the calcium buffered by the mitochondria during the influx of calcium during glutamate stimulation. This calcium released into the cytosol is then detected by the Mag-Fura 2. This provided an estimation of the mitochondria's calcium buffering abilities and a way of comparing the physiological impact between the two groups.

For these experiments the perfusion time course went as follows: approximately 7.5 minutes with HBSS, 5 minutes with 30 µM Glutamate/1 µM Glycine, 10 minutes with HBSS, then finally 5 minutes with 750 nM FCCP. A typical course of 340/380 ratios observed over the duration of the experiment possessed the following characteristics

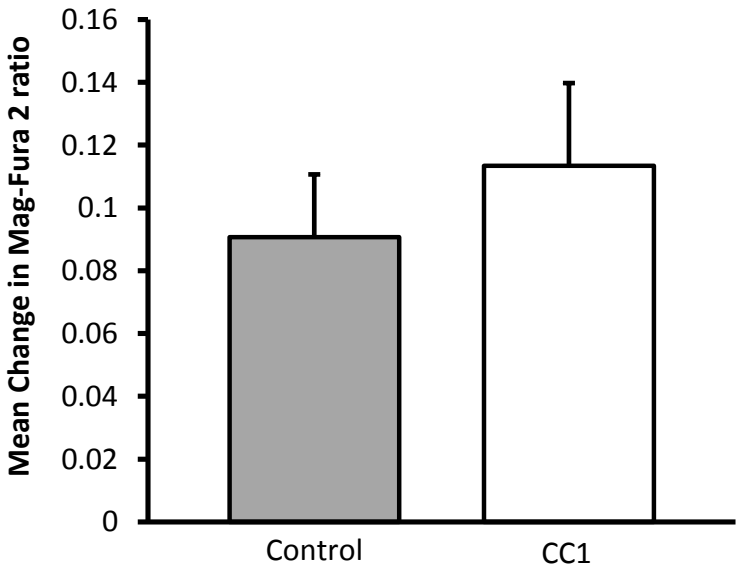

Figure 3.13: CC1 had no significant effect on the change in Mag-Fura 2 ratios during glutamate stimulation in cortical neurons.
Mean change in Mag-Fura 2 ratio during glutamate stimulation were determined for controls and CC1 neurons. Values were obtained by measuring the highest mag-fura 2 ratio observed during glutamate stimulation and subtracting the baseline mag-fura 2 ratio. Mean peak calcium was not significantly different between the control and CC1 neurons ($p=0.49$ using student's t-test; control, n=18 cells; CC1, n=20 cells). Values expressed as means ± S.E.M.

(figure 3.12): a stable baseline during HBSS perfusion, an increase during glutamate stimulation, recovery to near-baseline levels during the recovery period of HBSS perfusion after glutamate stimulation, and finally a large increase during FCCP stimulation. From this trace, we calculated the following parameters to assess the mitochondria's calcium buffering abilities: change in Mag-Fura 2 ratio during glutamate stimulation, change in Mag-Fura 2 ratio during FCCP stimulation, AUC during glutamate stimulation, AUC during FCCP stimulation, and a ratio of FCCP AUC to glutamate AUC.

Change in Mag-Fura 2 ratio during glutamate and FCCP stimulation was baseline-subtracted and indicates the relative maximum calcium levels obtained during the respective stimulation. AUC during glutamate and FCCP stimulation measures the total relative changes in intracellular calcium levels during the different treatments. Ratios of FCCP to glutamate AUC reveal the proportion of which changes in intracellular calcium levels are buffered by mitochondria. The mean change in Mag-Fura 2 ratios observed during glutamate stimulation in cortical neurons transfected with and without CC1 is summarized in figure 3.13. The CC1 transfected cells (0.113 ± 0.026, N=20 cells) did not show a significant difference in the mean change in Mag-Fura 2 ratio during glutamate stimulation compared to controls (0.091 ± 0.020, N=18 cells; p=0.49; t-test).

The mean change in Mag-Fura 2 ratio during FCCP stimulation (figure 3.14) showed the same trend with the controls (0.366 ± 0.043, N=18 cells) not significantly different from the CC1 transfected cells (0.276 ± 0.034, N=20 cells; p=0.11; t-test). The AUC during glutamate stimulation was not significant between groups (figure 3.15); 60.23 ± 2.29 (N=18 cells) for the controls and 60.24 ± 1.14 (N=20 cells; p=0.99; t-test) for the CC1 cells. The AUC during FCCP stimulation also show now significant change from between groups (figure 3.16); the controls with a mean of 113.50 ± 8.29 (N=18 cells) and the CC1 cells with a mean of 96.72 ± 5.19 (N=20 cells; p=0.09; t-test). The ratio of FCCP AUC to glutamate AUC, however, showed a significant difference between groups (figure 3.17). The controls had a greater mean ratio at 1.872 ± 0.097 (N=18 cells) compared to the CC1 cell's mean, 1.604 ± 0.078 (N=20 cells; $p<0.05$; t-test). These results suggest that CC1 significantly decreases the calcium uptake of mitochondria.

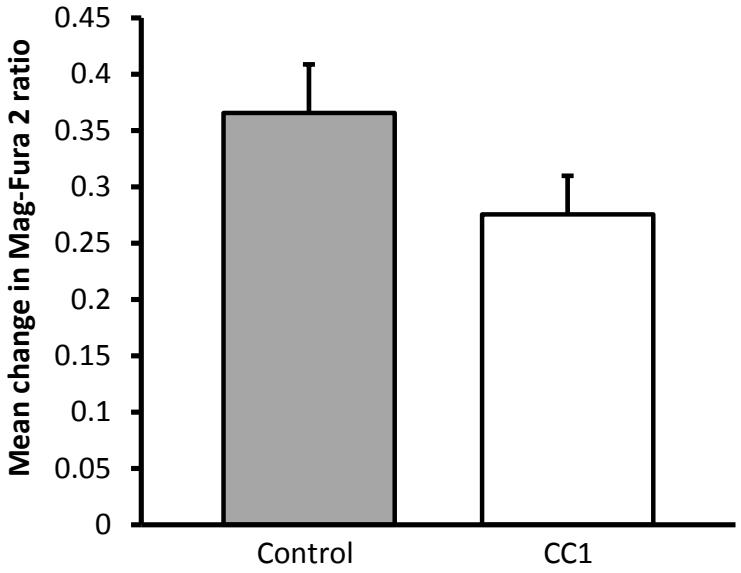

Figure 3.14: CC1 had no significant effect on the change in Mag-Fura 2 ratio during FCCP stimulation in cortical neurons.
Mean change in Mag-Fura 2 ratio during FCCP stimulation were determined for controls and CC1 neurons. Values were obtained by measuring the highest mag-fura 2 ratio observed during FCCP stimulation and subtracting the baseline mag-fura 2 ratio. Mean peak calcium was not significantly different between the control and CC1 neurons (p=0.11 using student's t-test; control, n=18 cells; CC1, n=20 cells). Values expressed as means ± S.E.M.

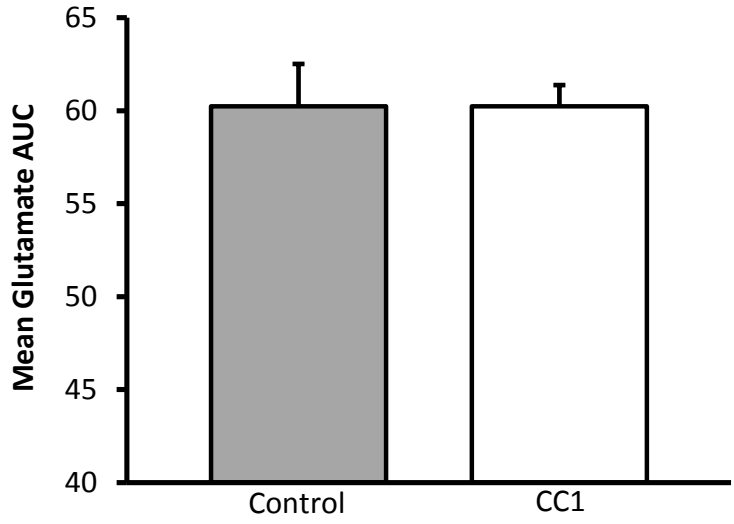

Figure 3.15: CC1 had no significant effect on AUC during glutamate stimulation in cortical neurons.
Mean AUC during glutamate stimulation was determined in control and CC1 neurons. Values were obtained by adding the baseline-subtracted mag-fura 2 ratios over the course of the glutamate treatment. Control AUC was not significantly different from the CC1 group (p=0.99 using student's t-test; control, n=18 cells; CC1, n=20 cells). Values expressed as means ± S.E.M.

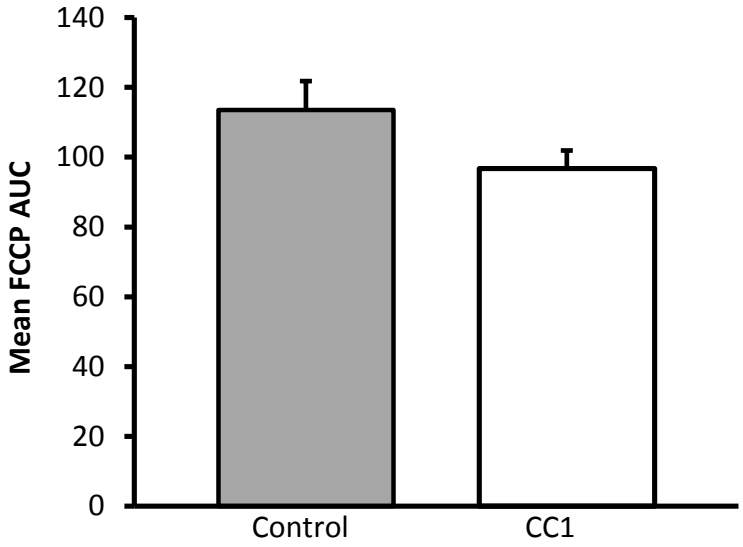

Figure 3.16: CC1 had no significant effect on AUC during FCCP stimulation in cortical neurons.
Mean AUC during FCCP stimulation was determined in control and CC1 neurons. Values were obtained by adding the baseline-subtracted mag-fura 2 ratios over the course of the glutamate treatment. Control AUC was not significantly different from the CC1 group (p=0.09 using student's t-test; control, n=18 cells; CC1, n=20 cells). Values expressed as means ± S.E.M.

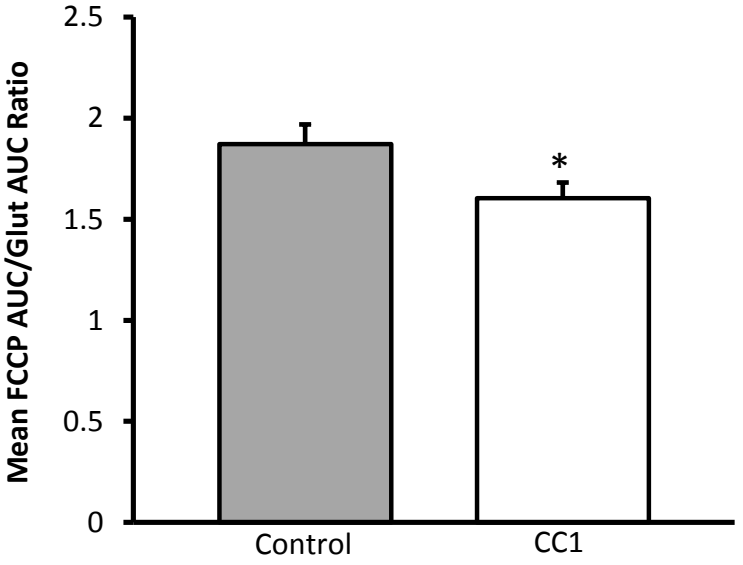

Figure 3.17: CC1 significantly decreased the ratio of FCCP to Glutamate AUC in cortical neurons.
Ratios of FCCP/Glut AUCs were determined in control and CC1 neurons. Values were obtained by dividing the FCCP AUC by the glutamate AUC. The CC1 cells had a significantly reduced ratio when compared to the controls ($p<0.05$ using student's t-test; control, n=18 cells; CC1, n=20 cells). * denotes a significant difference from controls. Values expressed as mean ± S.E.M.

3.4 Mitochondrial Membrane Potential

Previous studies of mitochondrial physiology have assessed the ΔΨm due to its integral connection to cellular respiration and ATP production (as reviewed by Duchen, 2004). Therefore, the effect of CC1 on the ΔΨm was examined. For these experiments TMRM was used. The dye is taken up by the mitochondria in proportion to ΔΨm and is quenched within the mitochondria, in which the dye exhibits a fairly low level of fluorescence intensity. Once released into the cytoplasm, which we induced by exposing cells to FCCP which dissipates the ΔΨm, the fluorescence intensity increases. This increase in fluorescence intensity after FCCP exposure was measured. Because the amount of dye present within the mitochondria is proportional to ΔΨm, the change in intensity after FCCP stimulation provides us with a method of measuring ΔΨm.

Cells were perfused with HBSS + 0.02 nM of TMRM when imaging. After 7 minutes the cells were exposed to 750 nM of FCCP to release the dye sequestered in the mitochondria. A typical graph of fluorescence intensities over the course of the experiment using TMRM possesses the following characteristics: a stable baseline, an increase in fluorescence intensity after FCCP stimulation, and a drop in fluorescence intensity after the peak intensity is reached (figure 3.18). We measured this increase by subtracting the baseline fluorescence (F_o) from the maximum fluorescence intensity (F_f) to obtain the change in fluorescence (ΔF), and then dividing ΔF by the baseline fluorescence (F_o) to normalize for the variability in baseline fluorescence. From these measurements and calculations, we reported ΔΨm as $\Delta F/ F_o$. The mean $\Delta F/ F_o$ values observed with TMRM are summarized in figure 3.19. In neurons loaded with TMRM, the controls had a significantly larger mean $\Delta F/ F_o$ at 0.395 ± 0.036 (n=30 cells) compared to a mean of 0.293 ± 0.031 (n=25 cells; $p<0.05$; t-test) observed for the CC1 cells. From this experiment, it is apparent that ΔΨm is significantly decreased in the CC1 transfected cells.

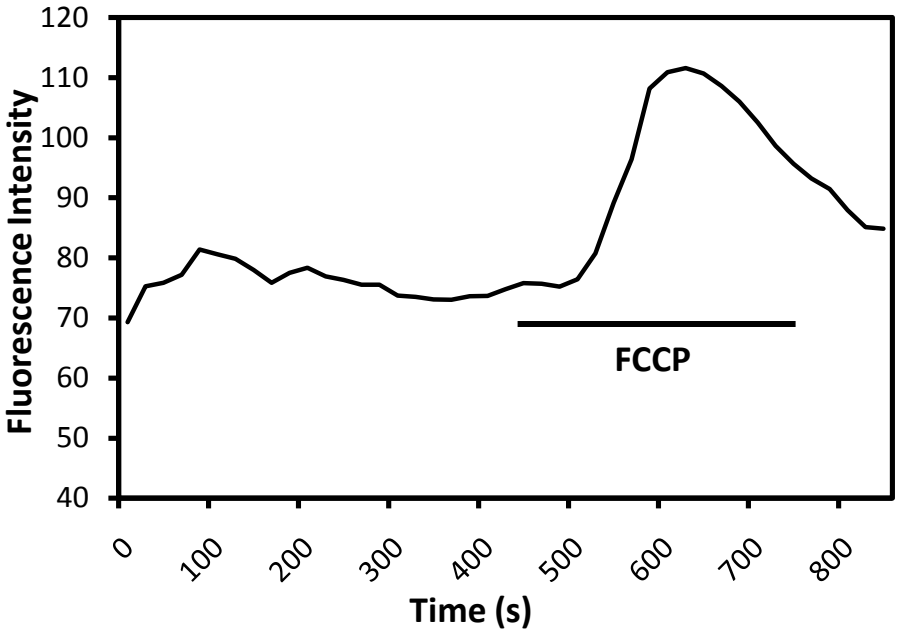

Figure 3.18: Measuring mitochondrial membrane potential in cortical neurons.
ΔΨm was assessed in control and CC1 neurons using TMRM. Cells included in analysis showed a similar trend in fluorescence intensity: a stable baseline; and increase in intensity, reaching a peak during FCCP stimulation; and a decrease in intensity following the peak. Cells that did not respond to FCCP stimulation were not included. $\Delta F/ F_o$ was determined and indirectly indicated the ΔΨm

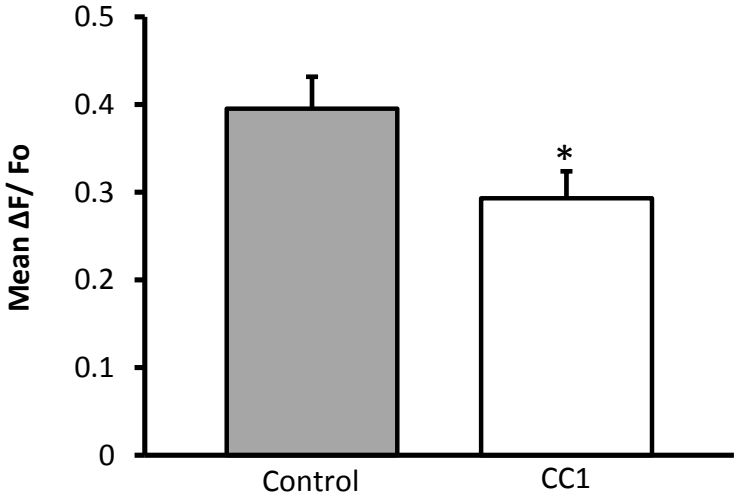

Figure 3.19: CC1 significantly decreased mitochondrial membrane potential in cortical neurons.
Mean ΔΨm, expressed as $\Delta F/ F_o$ was determined for control and CC1 neurons. CC1 cells showed a significant decrease in ΔΨm compared to controls ($p<0.05$ using student's t-test; control, n=30 cells; CC1, n=25 cells). * denotes a significant difference from controls. Values expressed as mean ± S.E.M.

3.5 Cell Survival

In the final set of experiments, the global effect of CC1 on cell viability and the impact of CC1 expression on cell survival survival following a glutamate challenge was investigated. To address this question, three different treatment conditions were set up for each group; a positive control, a negative control, and the glutamate treatment. In each condition, the numbers of CFP positive cells present in three adjacent rectangular areas that span the vertical diameter of the coverslip were counted. For the positive controls, the cells were treated with 250µM glutamate + 1µM glycine overnight to ensure cell death. The glutamate treatment group was exposed to 30 µM glutamate + 1µM Glycine while the negative controls were rinsed with HBSS and were used to obtain the cell viability in the absence of a glutamate challenge and used in conjunction with the glutamate treatment to calculate cell survival in the presence of a glutamate challenge (% survival). It is apparent that CC1 has an effect on cell viability and health since the mean number of CFP positive cells present in the controls (80.95 ± 22.49 cells, N=19 coverslips) is significantly larger than the mean number of CFP positive cells present in the CC1 transfected cells (20.63 ± 5.16 cells, N=19 coverslips; $p<0.05$; t-test) (figure 3.20); however, when looking at cell survival after glutamate challenge (figure 3.21), there was no significant difference in the percent survival between the controls and CC1 transfected cells. The controls had a mean survival rate of 66.62 ± 6.47% (N=9 cells) while the CC1 cells had a mean survival rate of 65.62 ± 10.60% (N=9 cells; $p=0.93$; t-test). From this data, it is apparent that CC1 has a significant effect on cell viability (however, see discussion) and health, however, does not have any impact on the cells' ability to recover from a glutamate challenge.

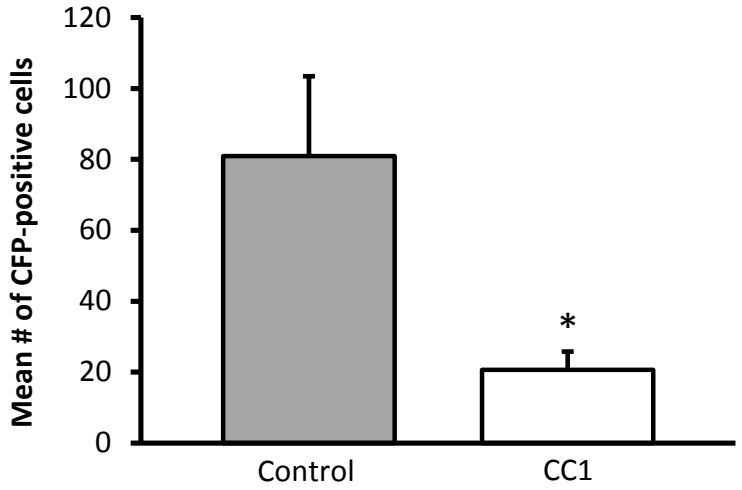

Figure 3.20: CC1 significantly reduced neuronal viability.
Cell viability, expressed as the mean number of CFP-positive cells (cells that are viable) was assessed in controls and CC1 neurons**.** Cells in three adjacent rectangular areas that span the vertical diameter of the coverslip were counted in controls and CC1 cells. CC1 neurons showed significantly lower viability compared to the controls ($p<0.05$ using student's t-test; control, n=19 coverslips; CC1, n=19 coverslips). * denotes a significant difference from controls. Values expressed as mean ± S.E.M.

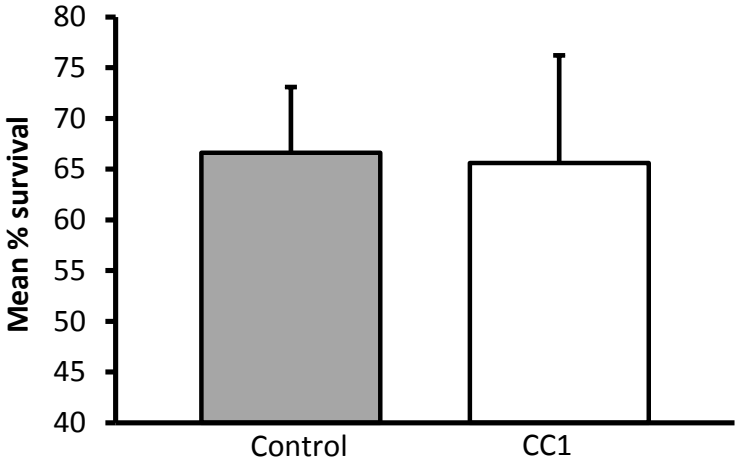

Figure 3.21: CC1 had no significant effect on neuronal survival rate following glutamate challenge.
Cell survival rate following a glutamate challenge, expressed as percent survival was determined in control and CC1 neurons. CFP- positive cells (viable cells) in three adjacent rectangular areas that span the vertical diameter of the coverslip were counted in controls and CC1 cells. Values were obtained by dividing the number of CFP-positive cells present on a coverslip after a glutamate challenge by the number of CFP-positive cells present on the negative control coverslip. There was no significant difference in survival rates between the two groups ($p=0.93$ using student's t-test; control, n=9 coverslips; CC1, n=9 coverslips). Values expressed as mean ± S.E.M.

4 CONCLUSIONS AND DISCUSSION

4.1 Summary of Findings

This project examined and characterized some of the effects of CC1 overexpression on mitochondrial dynamics. Effects on mitochondrial morphology, motility, and trafficking in astrocytes and cortical neurons and some aspects of mitochondrial physiology in primary cortical neurons were examined. No previous studies have investigated the effect of CC1 on mitochondrial dynamics and physiology.

Overexpression of CC1 in both astrocytes and cortical neurons had a dramatic effect on mitochondrial morphology and motility. With respect to mitochondrial morphology, CC1 caused a significant decrease in length transforming them from elongated, thread-like filamentous mitochondria to relatively small punctate mitochondria (figure 3.1 & 3.3). In terms of mitochondrial motility, significant reductions in movement were observed. In astrocytes and cortical neurons transfected with CC1, mitochondrial movement was significantly reduced to approximately half of basal motility levels (figure 3.5 & 3.6). The trafficking of mitochondria, however, was affected differently in astrocytes versus cortical neurons. Mitochondria in astrocytes expressing CC1 exhibited a more perinuclear localization (figure 3.1 & 3.2) while mitochondria in cortical neurons expressing CC1 had no significant alteration in the distribution of mitochondria along the neuronal process (figure 3.8). When further inspection of mitochondrial trafficking in primary cortical neurons was performed, interesting deficiencies were observed. In primary cortical neurons transfected with CC1, both retrograde and anterograde transport were significantly reduced by approximately 60% (figure 3.10). Based on these observations, we concluded that CC1 disrupted mitochondrial motility and induced changes in mitochondrial trafficking in neurons and astrocytes.

Significant changes in mitochondrial physiology were also observed in cortical neurons transfected with CC1. The particular physiological parameters of mitochondria we investigated were calcium buffering and ΔΨm. With respect to mitochondrial calcium buffering, a significant decrease in the amount of calcium buffered specifically by mitochondria was observed. This fact can be seen in the decreased ratio of glutamate-stimulated AUC to FCCP-stimulated AUC (figure 3.17). These observations lead us to believe that the amount of calcium taken up by mitochondria is significantly reduced in neurons with reduced mitochondrial transport. ΔΨm, another essential parameter that is involved in cellular respiration and ATP synthesis, was also decreased in neurons overexpressing CC1 (figure 3.19). Collectively, these results suggest that disruptions of mitochondrial transport have an impact on their physiological state.

Finally, the effect of CC1 on basal cell viability and survival after exposure to a glutamate challenge was investigated. In cells transfected with CC1, the mean percent viability was significantly decreased when compared to controls (figure 3.20). Mean percent survival after a glutamate challenge, on the other hand, showed no significant difference (figure 3.21). These results suggest that expression of CC1 itself leads to deficiencies in normal cell function and trigger an increased death rate (but see below); however, it does not exacerbate neuronal injury in glutamate toxicity models.

Clearly there is an impact on mitochondrial dynamics when their transport is disrupted. CC1 has an apparent effect on mitochondrial morphology, motility, and trafficking. It also has a significant effect on mitochondrial physiology and perhaps basal cell viability.

4.2 Mitochondrial Morphology

Mitochondrial morphology is a highly regulated process that is controlled by proteins such as Drp1, Mfn1, and Mfn2 (as reviewed by Liesa et al., 2009) and the balance between the actions of these proteins determines the shape of the mitochondria. The morphology of mitochondria within astrocytes and cortical neurons

in response to disruption of transport via overexpression of CC1 was examined. Results show that there is a significant change in the morphology of neurons expressing CC1. In astrocytes and neurons, the mitochondria are elongated under normal conditions; however, when CC1 is expressed the mitochondria become short and punctate.

This change in morphology could be due to a change in the balance of mitochondrial fission and fusion. It is widely accepted that mitochondrial fusion and fission proteins and the balance between the two, control overall mitochondrial shape (as reviewed by Liesa et al., 2009). In this case, there could be some effect on the expression of these proteins in response to a disruption in movement. Since Drp1 has been reported in numerous studies to regulate mitochondrial fission (Labrousse et al., 1999), CC1 may increase the expression of Drp1, causing an increase in the fission rate. This increase in Drp1 activity would lead to smaller mitochondria, as seen in experiments where overexpression of Drp1 lead to fragmented mitochondria (Barsoum et al., 2006). Conversely, the possibility exists that CC1 can affect the expression of fusion proteins Mfn1 and Mfn2. Due to the fact that Mfn1 and Mfn2 control mitochondrial fusion (Santel and Fuller, 2001), decreases in their expression could initiate a decrease in fusion, giving mitochondria a more fragmented morphology. In other words, CC1 could perturb the function of Mfn1 or Mfn2, causing a decrease in the amount of mitochondria fusion that occurs, shifting the fission/fusion balance towards mitochondrial fission. Both explanations could account for the observed change in mitochondrial shape. However, the results that will be discussed in subsequent sections suggest that changes in fission/fusion dynamics may not be responsible for the observed changes in mitochondrial morphology.

Another mechanism that can explain these changes in mitochondrial morphology may be linked to their decrease in motility. As stated above, mitochondrial morphology is controlled by the balance between the activity of fusion (Mfn1, Mfn2, and OPA1) and fission (Drp1) proteins (as reviewed by Liesa et al., 2009; Rintoul and Reynolds, 2009). Therefore, in order for two different mitochondria to undergo fusion, contact between them is required before fusion can occur. In cells transfected with CC1 the amount of

mitochondrial movement measured decreased significantly (figure 3.5 & 3.6). Therefore, if the motility of mitochondria is significantly decreased, then the probability of two separate mitochondria coming into close proximity to one another would be lower compared to controls. Given that contact between mitochondria is required for fusion and assuming all fission/fusion proteins are present at normal levels, the decreased mobility of mitochondria could indirectly decrease fusion since the probability of two mitochondria coming in contact is decreased. In turn, fission would continue, leading to more punctate mitochondria.

When neurons overexpressed CC1, dramatic changes in mitochondrial morphology were observed; however, when the distribution of mitochondria along a neuronal process was investigated, the results suggested that this morphological change may not be a product of fission/fusion imbalances. Examination of mitochondrial distribution showed that the area of neuronal process that was occupied by mitochondria significantly decreased compared to controls (figure 3.9). Upon initial inspection, it appeared that this could be a result of either trafficking defects or fission/fusion imbalances; however, when coupled with data on the mitochondrial length and number of mitochondria, it appears that this is not the case. In cortical neurons expressing CC1, there was a significant decrease in mitochondrial length (figure 3.4); however, there were no significant differences in the number of mitochondria per µm of neuronal process (figure 3.8). These results suggest that the changes in mitochondrial morphology are a result of mitochondrial remodelling and not fission/fusion imbalances.

Previous studies have also observed rounding of mitochondria in response to increased intracellular calcium levels and they suggested that this was a result of mitochondrial permeability transition (mPT) (Crompton et al., 1988; Kristal and Dubinsky, 1997). The mPT is characterized by the opening of a pore within the inner mitochondria membrane in response to high levels of intracellular calcium, allowing free diffusion of solutes from the mitochondrial matrix into the intermembrane space. This results in uncoupling of respiration and collapse of the $\Delta\Psi m$, contributing to cell death

(Kristal and Dubinsky, 1997). This may explain the observed changes in mitochondrial morphology; however, the experimental procedures used when examining morphology were different and were unlikely to have induced mPT. In the experiments that characterize mitochondrial morphology, neurons and astrocytes were never exposed to conditions that induced heightened levels of intracellular calcium as in the study done by Kristal and Dubinsky (1997). In addition, the mitochondrial permeability transition appears to be a toxic and devastating event that is believed to be an upstream event in cell death. It is unlikely that the rounding observed in CC1-transfected cells is due to mPT as the cells appear otherwise healthy and exhibited robust recovery from glutamate challenge.

Another possible explanation for the change in mitochondrial morphology may be related to motor proteins and mitochondrial motility. In CC1 transfected cells, mitochondrial movement, which will be discussed in detail in the following section, was significantly decreased. In cells with normal functioning motor proteins, the motors may be involved in actively stretching the mitochondria along the cytoskeletal tracks. Once that control is disrupted or inactive, the mitochondria may contract to a more spherical and punctate shape.

4.3 Mitochondrial Motility and Trafficking

It is generally accepted that mitochondria are mobile structures in both astrocytes and neurons. Although the significance of this is largely unexplored, it is believed that cells transport mitochondria to distal areas of the cell that require large amounts of energy or calcium buffering. Areas such as synapses and nodes of Ranvier (Palay, 1956; Fabricius et al., 1993) have a high metabolic demand and require a local source of ATP to meet that demand. In our experiments, we used CC1 to disrupt mitochondrial movement in astrocytes and cortical neurons. CC1 overexpression is established as a reliable means of disrupting dynein function in cells (Quintyne et al., 1999). CC1 is the first coiled-coil region of the $p150^{Glued}$ subunit of the dynactin complex

(Quintyne et al., 1999). This region is considered dynactin's dynein binding sequence; therefore, overexpression of CC1 will bind cytoplasmic dynein and prevent the recruitment of dynein to endogenous functional dynactin. The purpose of this experiment was to characterize basic movement parameters of mitochondria in response to CC1 expression. Results show that there is a significant decrease in movement in both astrocytes and neurons transfected with CC1 (figures 3.5 & 3.6). In addition, this disruption is not specific to mitochondria. The movement of NPY vesicles in neurons were also significantly decreased in cells transfected with CC1 (figure 3.11). These results were consistent with the hypothesis that CC1 would decrease mitochondrial movement.

Mitochondrial trafficking was then characterized in response to CC1 overexpression. With respect to mitochondrial motility, it is important to differentiate between mitochondrial movement and mitochondrial trafficking. Trafficking of mitochondria refers to the movement of mitochondria in a particular direction, either anterograde or retrograde, leading to varying distributions of mitochondria within the cell, either more or less mitochondria in the periphery of the cell or in the cell body. In terms of movement, a mitochondrion may be moving but not necessarily trafficked. This is referred to as mitochondrial 'wiggling' or oscillation, where the mitochondria are moving back and forth within a small area. As few previous studies have documented such events (Rintoul et al., 2003), its importance to cellular physiology is largely unexplored. To assess the effect of CC1 on mitochondrial trafficking in astrocytes and neurons, images of CC1-transfected cells were analyzed and the distribution of mitochondria within the cells was compared.

Within astrocytes, the distribution of mitochondria was significantly affected by dynein/dynactin disruption. In CC1-transfected cells, the majority of mitochondria were located perinuclearly. The controls, on the other hand, had an even distribution of mitochondria (figures 3.1 3.7). Since the arrangement of microtubules in astrocytes remains unclear, it is difficult to explain the changes in mitochondrial distribution in response to CC1 overexpression. However, one possibility is that the microtubules may

be organized such that the 'minus'-end of the filament is pointed towards the periphery and the 'plus'-end is pointed towards the nucleus. Since CC1 disrupts the activity of dynein motors, a minus-end directed motor, a more perinuclear distribution would result. Although mitochondrial transport in astrocytes may be significant, it has not received as much attention as neurons. Mitochondrial transport in astrocytes and the machinery involved merits further investigation.

In CC1-transfected neurons, the distribution of mitochondria within the processes remained unchanged. The number of mitochondria along a process was not significantly different from the controls (figure 3.8); however, the mitochondria occupied a significantly smaller percentage of the process due to the decrease in length (figures 3.9 & 3.4). In addition, there was a significant decrease in the number of trafficked mitochondria within a process of cells transfected with CC1 (figure 3.10). In cortical neurons transfected with CC1, the number of mitochondria moving in the retrograde and anterograde direction was significantly reduced. This can be explained by the effect of CC1 on dynein activity and the microtubule organization in dendrites. In proximal dendrites, the polarity of microtubules is mixed; the minus-end of the microtubule can point to either the cell periphery or the cell body (as reviewed by Hirokawa and Takemura, 2005). Therefore, due the mixed polarity of microtubules in proximal dendrites (Burton and Paige, 1981; Baas et al., 1988), a reduction in dynein activity, through CC1 overexpression, would affect the movement of mitochondria in both directions. However, within axons where the polarity of microtubules is uniform (Burton and Paige, 1981; Baas et al., 1988) the changes is mitochondrial trafficking would not be explained by the microtubule organization. Studies have reported that organelles that undergo bidirectional movement in axons due to opposing motors bound at any given time. The cooperation of the two motors determines the net movement of that organelle (Deacon et al., 2003; Colin et al., 2008). In another study conducted by Ally et al. (2009), they reported that in order for KIF5 to function normally, dynein must be fully functional and bound to the same organelle, and vice versa. Therefore, in this case where a significant reduction in retrograde and anterograde

movement was observed, the probable explanation is that CC1 overexpression disrupts dynein recruitment to the organelle, which not only disrupts retrograde movement but disrupts anterograde movement as well, compromising the function of both KIF5 and KIF1Bα motors.

4.4 Mitochondrial Physiology

Proper mitochondrial physiology is absolutely essential to neuronal health and survival. Mitochondria produce by far the largest amount of ATP in the cell and they do so with a high degree of efficiency (as reviewed by Chang and Reynolds, 2006). In addition, they play a vital role in regulating intracellular calcium levels (as reviewed by Hollenbeck and Saxton, 2005). Both of these functions are closely linked to the ΔΨm: an electrochemical potential that arises from the differences in ion concentrations generated across the inner mitochondrial membrane. In these experiments, the effect of CC1 on mitochondrial physiology was assessed by examining the calcium buffering and the ΔΨm of the cells.

Previous studies have used calcium-sensitive dyes such as Mag-Fura 2 to monitor intracellular calcium levels (Brocard et al., 2001). In their experiments, they induced influx of extracellular calcium into the cell with glutamate mainly through the activation of NMDA receptors (Brocard et al., 2001). After a recovery period, cells were then treated with FCCP to release the calcium sequestered in mitochondria. Similar procedures to those used by Brocard et al. (2001) were used to investigate mitochondrial calcium dynamics in the presence of CC1 overexpression. When comparing the controls and CC1-transfected cells, the only parameter that was significantly different in the CC1-transfected cells was the ratio of FCCP-stimulated AUC to glutamate-stimulated AUC (F/G AUC ratio) (figures 3.13 to 3.17). When anaylzing Mag-Fura 2 traces, the AUC provides an estimation of the total changes in intracellular calcium concentration that occurred during a particular treatment. In CC1 cells, the F/G AUC ratio was significantly decreased when compared to controls (figure 3.18). This

suggests that CC1 decreased the proportion of calcium buffered by mitochondria. The movement of calcium into mitochondria is mediated by a calcium uniporter and is driven by the ΔΨm (Duchen, 2004). Therefore, decreases in the amount of calcium taken up by mitochondria could be a result of compromises in either the ΔΨm or the function of the calcium uniporter; since mitochondrial calcium accumulation is very sensitive to the voltage across the mitochondrial membrane, it is likely that this oberservation is a result of a decreased potential across the mitochondrial membrane. If this is the case, then CC1 should also have a significant effect on ΔΨm.

The electrochemical gradient known as the ΔΨm, present across the mitochondrial membrane is important in mitochondrial processes such as ATP synthesis and calcium buffering (as reviewed by Duchen, 2004). This is evident in cases, such as glutamate-mediated excitotoxicity, where dissipation of the ΔΨm leads to the increased production of ROS and eventual cell death (as reviewed by Mattson, 2003). Therefore, to assess the effect of CC1 on mitochondrial physiology, changes in ΔΨm in response to CC1 overexpression were examined. In cells transfected with CC1, ΔΨm was significantly reduced (figure 3.20). The most probable explanation for these findings may be linked to the morphology of the mitochondria in response to CC1 overexpression. Our results described above have shown a clear affect on mitochondrial morphology. In CC1-transfected cells, mitochondria were more punctate and rounded and did not resemble the long, 'worm-like' morphology in controls (figures 3.1 & 3.3). This change in mitochondrial morphology could possibly translate into changes in ΔΨm. Previous studies have suggested that longer mitochondria possess an advantage over punctate mitochondria because they can provide energy for a larger cellular area, conduct ΔΨm to other mitochondria and locations, and minimize the amount of energy lost during respiration (Skulachev, 2001). Previous studies have shown that disruptions in mitochondrial fusion lead to a decrease in ΔΨm (Pich et al., 2005). Therefore, if disrupting transport via CC1 alters mitochondrial morphology, then the result could be a decreased ΔΨm. A reduced membrane potential due to CC1-mediated effects would be consistent with the finding that mitochondria in CC1 transfected cells exhibit a

significantly decreased calcium uptake during glutamate stimulus. Experiments examining intracellular ATP and oxygen consumption would provide further insight into the links between fission/fusion and the bioenergetic state of mitochondria.

4.5 Cell Viability and Survival

In the previous section the effect on CC1 on mitochondrial dynamics was examined. In subsequent experiments, the impact of these perturbations on viability and survival after a glutamate challenge were investigated. Viability addressed the effect of CC1 on overall cell health while survival after glutamate challenge addressed the ability of transport-disrupted mitochondria to survive in an injury paradigm.

With respect to survival after glutamate challenge, rates of survival were not significantly different between controls and CC1-transfected cells (figure 3.22). The main mechanism at work in this experiment is glutamate-mediated excitotoxicity. Control and CC1-transfected cells were exposed to concentrations of glutamate that are high enough to cause excitotoxic cell death and survival rates of both groups were not significantly different (figure 3.22); suggesting that disrupting transport of mitochondria does not alter susceptibility to glutamate-mediated excitotoxocity. However, it is possible that the proportion of cells that survive is relatively equal but the cells die from excitoxicity do so at 12 hours after exposure instead of 24-48 hours after exposure. Under normal conditions, cell death from glutamate excitoxicity occurs within 24-48 hours after glutamate exposure due to the series of events, such as collapse of the $\Delta\Psi m$ and subsequent release of ROS and apoptotic factors (as reviewed by Mattson, 2003). In the case of CC1 cells, it is possible that the time it takes for the $\Delta\Psi m$ to collapse may be less than in untransfected controls, thus allowing the cascade to proceed faster than normal. However, the design of the experiment would not be able to detect this. Looking at cell survival rates at different time intervals would address this issue. Another possible explanation that could account for the similar survival rate is the concentration of glutamate the cells are exposed to. Perhaps 30µM glutamate leads to cell death in

healthy and compromised cells because the concentration was too high for any cell to handle. One way to address this issue would be to perform the glutamate challenge experiments with different concentrations of glutamate, producing a dose-dependent curve of cell survival. It is possible that at a lower concentration of glutamate transport disrupted cells may be more sensitive to glutamate challenge while control cells would be able to recover.

In contrast, CC1 had an effect on overall neuronal health. Neuronal viability was significantly reduced in cells transfected with CC1 when compared to controls. In this case, disruption of dynactin compromised cell health resulting in an increased rate of cell death. There are two possible explanations for these observations: 1) the difference in CFP-positive or viable cells could be a result of the different transfection efficiencies of the cytosolic CFP and CC1 or 2) CC1 overexpression results in increased cell death. There is a possibility that these findings may be attributed to differential transfection of different plasmids. The cytosolic CFP and CC1 plasmid are different constructs and there may be a difference in the efficiency of its uptake into the cell during the transfection process. In addition, there was no other parameter that we could use to normalize for transfection efficiency of the constructs; therefore, raw counts of CFP-positive cells were obtained for each cell. If the CC1 plasmid was less likely to be taken up by the cell due to its larger size for example, then this significant decrease in viability would be merely a manifestation of differing transfection efficiencies of the two different plasmids used. Assuming the transfection efficiencies of the two constructs was not significantly different; the overexpression of CC1 causes an increase mortality rate. Although this experiment suggests a clear decrease in cell viability, it does not specifically address the effect of *mitochondrial* transport disruption on cell viability. Given that overexpression of CC1 affected other cargo as well, it remains unclear whether this observation is attributed to mitochondria-specific transport defects or the global disruption of transport in the cell. In other words, the effect that we observed may not be a result of mitochondrial transport defects and that it is possibly a consequence of transport defects of all organelles and not just mitochondria. The failure

of mitochondria to provide the distal regions with sufficient ATP for normal function may be a significant contributor to cell death; however, it is possible that defects in the transport of other organelles are contributing as well. If proteins that are normally brought back to the cell body for degradation are not cleared, protein aggregates can form, creating a 'log jam' causing further obstacles for transport. Simultaneously, essential resources and proteins needed to maintain the distal regions such as synapses are not delivered, leading to perturbations of cell homeostasis and synaptic dysfunction. A future experiment to perform that could address the specific contribution of mitochondrial translocation and trafficking would be disrupting adaptor proteins that are specific to mitochondria, such as miro/Milton via overexpression of mutant adaptor proteins or siRNA specific to mitochondrial motor/adaptor proteins. In this situation, only the transport of mitochondria would be affected and not other organelles. This would separate the importance of mitochondrial transport from the transport of other organelles, further elucidating the functional significance of mitochondrial transport to cell health and neuronal injury.

4.6 Conclusions and Future Directions

It is clear that transport disruption of mitochondria, through overexpression of CC1, has dramatic effects on mitochondrial morphology and physiology. Mitochondrial movement was significantly reduced in both astrocytes and neurons. The reductions in mitochondrial movement lead to changes in mitochondrial morphology; however, the exact mechanism that links the two events remains unclear. It would be interesting to look at the effect of transport on fission/fusion protein activity. This would address the morphological changes observed when mitochondrial transport is disrupted. In addition, it would provide some insight into the mechanisms responsible for this change in morphology; whether it is a result of changes in fission/fusion expression or mitochondrial 'remodelling' reported in other studies (Rintoul et al., 2003). These morphological changes also resulted in perturbed mitochondrial physiology. In CC1-

transfected cells, ΔΨm and mitochondrial calcium uptake were significantly reduced. Seeing as ΔΨm is significantly reduced in CC1-overexpressing cells, it would be worthwhile to examine the effects of CC1 on ATP production and ROS generation. Ultimately, these changes in morphology and physiology may lead to an increase in cell mortality. However, the contribution of mitochondrial transport disruption to cell death remains unanswered. Perhaps, experiments that specifically targeted mitochondrial transport mechanisms such as adaptor-motor complex disruption using siRNA specific to miro/Milton and syntabulin as stated above could provide some insight into this unexplored issue.

With respect to the main hypothesis of this thesis, CC1 did have a dramatic effect on mitochondrial dynamics as expected but not on cell survival. When movement of mitochondria was disrupted, significant changes in mitochondrial dynamics were observed; dramatic changes in mitochondrial morphology and trafficking were a result of dynein/dynactin disruption. In addition, perturbations in mitochondrial movement reduced ΔΨm and mitochondrial calcium uptake. However, the impact of mitochondrial movement on survival after glutamate stress was not significantly affected. This suggests that, maintenance of mitochondrial motility and trafficking may not be critical in glutamate excitotoxicity, although further studies are required to confirm this hypothesis. These results have provided some insight as to the impact mitochondrial movement has on mitochondrial dynamics, physiology, and cell survival. Additional studies are merited to further characterize some of the mechanisms that link disruptions in mitochondrial movement to changes in mitochondrial dynamics, physiology, and cell survival.

REFERENCE LIST

Akepati, V. R., Muller, E. C., Otto, A., Strauss, H. M., Portwich, M. and Alexander, C. (2008). "Characterization of OPA1 isoforms isolated from mouse tissues." J Neurochem 106(1): 372-383.

Alexander, C., Votruba, M., Pesch, U. E., Thiselton, D. L., Mayer, S., Moore, A., Rodriguez, M., Kellner, U., Leo-Kottler, B., Auburger, G., Bhattacharya, S. S. and Wissinger, B. (2000). "OPA1, encoding a dynamin-related GTPase, is mutated in autosomal dominant optic atrophy linked to chromosome 3q28." Nat Genet 26(2): 211-215.

Ally, S., Larson, A. G., Barlan, K., Rice, S. E. and Gelfand, V. I. (2009). "Opposite-polarity motors activate one another to trigger cargo transport in live cells." J Cell Biol 187(7): 1071-1082.

Anandatheerthavarada, H. K., Biswas, G., Robin, M. A. and Avadhani, N. G. (2003). "Mitochondrial targeting and a novel transmembrane arrest of Alzheimer's amyloid precursor protein impairs mitochondrial function in neuronal cells." J Cell Biol 161(1): 41-54.

Arnoult, D., Grodet, A., Lee, Y. J., Estaquier, J. and Blackstone, C. (2005). "Release of OPA1 during apoptosis participates in the rapid and complete release of cytochrome c and subsequent mitochondrial fragmentation." J Biol Chem 280(42): 35742-35750.

Baas, P. W., Deitch, J. S., Black, M. M. and Banker, G. A. (1988). "Polarity orientation of microtubules in hippocampal neurons: uniformity in the axon and nonuniformity in the dendrite." Proc Natl Acad Sci U S A 85(21): 8335-8339.

Bach, D., Pich, S., Soriano, F. X., Vega, N., Baumgartner, B., Oriola, J., Daugaard, J. R., Lloberas, J., Camps, M., Zierath, J. R., Rabasa-Lhoret, R., Wallberg-Henriksson, H., Laville, M., Palacin, M., Vidal, H., Rivera, F., Brand, M. and Zorzano, A. (2003). "Mitofusin-2 determines mitochondrial network architecture and mitochondrial metabolism. A novel regulatory mechanism altered in obesity." J Biol Chem 278(19): 17190-17197.

Barsoum, M. J., Yuan, H., Gerencser, A. A., Liot, G., Kushnareva, Y., Graber, S., Kovacs, I., Lee, W. D., Waggoner, J., Cui, J., White, A. D., Bossy, B., Martinou, J. C., Youle, R. J., Lipton, S. A., Ellisman, M. H., Perkins, G. A. and Bossy-Wetzel, E. (2006). "Nitric

oxide-induced mitochondrial fission is regulated by dynamin-related GTPases in neurons." EMBO J 25(16): 3900-3911.

Benard, G., Bellance, N., James, D., Parrone, P., Fernandez, H., Letellier, T. and Rossignol, R. (2007). "Mitochondrial bioenergetics and structural network organization." J Cell Sci 120(Pt 5): 838-848.

Berezuk, M. A. and Schroer, T. A. (2007). "Dynactin enhances the processivity of kinesin-2." Traffic 8(2): 124-129.

Bingham, J. B. and Schroer, T. A. (1999). "Self-regulated polymerization of the actin-related protein Arp1." Curr Biol 9(4): 223-226.

Brickley, K., Smith, M. J., Beck, M. and Stephenson, F. A. (2005). "GRIF-1 and OIP106, members of a novel gene family of coiled-coil domain proteins: association in vivo and in vitro with kinesin." J Biol Chem 280(15): 14723-14732.

Bristow, E. A., Griffiths, P. G., Andrews, R. M., Johnson, M. A. and Turnbull, D. M. (2002). "The distribution of mitochondrial activity in relation to optic nerve structure." Arch Ophthalmol 120(6): 791-796.

Brocard, J. B., Tassetto, M. and Reynolds, I. J. (2001). "Quantitative evaluation of mitochondrial calcium content in rat cortical neurones following a glutamate stimulus." J Physiol 531(Pt 3): 793-805.

Budd, S. L. and Nicholls, D. G. (1996). "Mitochondria, calcium regulation, and acute glutamate excitotoxicity in cultured cerebellar granule cells." J Neurochem 67(6): 2282-2291.

Burton, P. R. and Paige, J. L. (1981). "Polarity of axoplasmic microtubules in the olfactory nerve of the frog." Proc Natl Acad Sci U S A 78(5): 3269-3273.

Cai, Q., Gerwin, C. and Sheng, Z. H. (2005). "Syntabulin-mediated anterograde transport of mitochondria along neuronal processes." J Cell Biol 170(6): 959-969.

Chang, C. R. and Blackstone, C. (2007). "Cyclic AMP-dependent protein kinase phosphorylation of Drp1 regulates its GTPase activity and mitochondrial morphology." J Biol Chem 282(30): 21583-21587.

Chang, D. T., Honick, A. S. and Reynolds, I. J. (2006b). "Mitochondrial trafficking to synapses in cultured primary cortical neurons." J Neurosci 26(26): 7035-7045.

Chang, D. T. and Reynolds, I. J. (2006). "Mitochondrial trafficking and morphology in healthy and injured neurons." Prog Neurobiol 80(5): 241-268.

Chang, D. T., Rintoul, G. L., Pandipati, S. and Reynolds, I. J. (2006). "Mutant huntingtin aggregates impair mitochondrial movement and trafficking in cortical neurons." Neurobiol Dis 22(2): 388-400.

Chang, S., ran Ma, T., Miranda, R. D., Balestra, M. E., Mahley, R. W. and Huang, Y. (2005). "Lipid- and receptor-binding regions of apolipoprotein E4 fragments act in concert to cause mitochondrial dysfunction and neurotoxicity." Proc Natl Acad Sci U S A 102(51): 18694-18699.

Chevalier-Larsen, E. and Holzbaur, E. L. (2006). "Axonal transport and neurodegenerative disease." Biochim Biophys Acta 1762(11-12): 1094-1108.

Choi, D. W. (1988). "Calcium-mediated neurotoxicity: relationship to specific channel types and role in ischemic damage." Trends Neurosci 11(10): 465-469.

Cingolani, L. A. and Goda, Y. (2008). "Actin in action: the interplay between the actin cytoskeleton and synaptic efficacy." Nat Rev Neurosci 9(5): 344-356.

Cleveland, D. W., Monteiro, M. J., Wong, P. C., Gill, S. R., Gearhart, J. D. and Hoffman, P. N. (1991). "Involvement of neurofilaments in the radial growth of axons." J Cell Sci Suppl 15: 85-95.

Colin, E., Zala, D., Liot, G., Rangone, H., Borrell-Pages, M., Li, X. J., Saudou, F. and Humbert, S. (2008). "Huntingtin phosphorylation acts as a molecular switch for anterograde/retrograde transport in neurons." EMBO J 27(15): 2124-2134.

Cribbs, J. T. and Strack, S. (2007). "Reversible phosphorylation of Drp1 by cyclic AMP-dependent protein kinase and calcineurin regulates mitochondrial fission and cell death." EMBO Rep 8(10): 939-944.

Crompton, M., Ellinger, H. and Costi, A. (1988). "Inhibition by cyclosporin A of a Ca2+-dependent pore in heart mitochondria activated by inorganic phosphate and oxidative stress." Biochem J 255(1): 357-360.

De Vos, K. J., Chapman, A. L., Tennant, M. E., Manser, C., Tudor, E. L., Lau, K. F., Brownlees, J., Ackerley, S., Shaw, P. J., McLoughlin, D. M., Shaw, C. E., Leigh, P. N., Miller, C. C. and Grierson, A. J. (2007). "Familial amyotrophic lateral sclerosis-linked SOD1 mutants perturb fast axonal transport to reduce axonal mitochondria content." Hum Mol Genet 16(22): 2720-2728.

Deacon, S. W., Serpinskaya, A. S., Vaughan, P. S., Lopez Fanarraga, M., Vernos, I., Vaughan, K. T. and Gelfand, V. I. (2003). "Dynactin is required for bidirectional organelle transport." J Cell Biol 160(3): 297-301.

Delettre, C., Griffoin, J. M., Kaplan, J., Dollfus, H., Lorenz, B., Faivre, L., Lenaers, G., Belenguer, P. and Hamel, C. P. (2001). "Mutation spectrum and splicing variants in the OPA1 gene." Hum Genet 109(6): 584-591.

Desai, A. and Mitchison, T. J. (1997). "Microtubule polymerization dynamics." Annu Rev Cell Dev Biol 13: 83-117.

Diefenbach, R. J., Mackay, J. P., Armati, P. J. and Cunningham, A. L. (1998). "The C-terminal region of the stalk domain of ubiquitous human kinesin heavy chain contains the binding site for kinesin light chain." Biochemistry 37(47): 16663-16670.

Duchen, M. R. (2004). "Mitochondria in health and disease: perspectives on a new mitochondrial biology." Mol Aspects Med 25(4): 365-451.

Duchen, M. R. (2004). "Roles of mitochondria in health and disease." Diabetes 53 Suppl 1: S96-102.

Ebneth, A., Godemann, R., Stamer, K., Illenberger, S., Trinczek, B. and Mandelkow, E. (1998). "Overexpression of tau protein inhibits kinesin-dependent trafficking of vesicles, mitochondria, and endoplasmic reticulum: implications for Alzheimer's disease." J Cell Biol 143(3): 777-794.

Echeverri, C. J., Paschal, B. M., Vaughan, K. T. and Vallee, R. B. (1996). "Molecular characterization of the 50-kD subunit of dynactin reveals function for the complex in chromosome alignment and spindle organization during mitosis." J Cell Biol 132(4): 617-633.

Eckley, D. M., Gill, S. R., Melkonian, K. A., Bingham, J. B., Goodson, H. V., Heuser, J. E. and Schroer, T. A. (1999). "Analysis of dynactin subcomplexes reveals a novel actin-related protein associated with the arp1 minifilament pointed end." J Cell Biol 147(2): 307-320.

Fabricius, C., Berthold, C. H. and Rydmark, M. (1993). "Axoplasmic organelles at nodes of Ranvier. II. Occurrence and distribution in large myelinated spinal cord axons of the adult cat." J Neurocytol 22(11): 941-954.

Fifkova, E. and Delay, R. J. (1982). "Cytoplasmic actin in neuronal processes as a possible mediator of synaptic plasticity." J Cell Biol 95(1): 345-350.

Gee, M. A., Heuser, J. E. and Vallee, R. B. (1997). "An extended microtubule-binding structure within the dynein motor domain." Nature 390(6660): 636-639.

Geraldo, S. and Gordon-Weeks, P. R. (2009). "Cytoskeletal dynamics in growth-cone steering." J Cell Sci 122(Pt 20): 3595-3604.

Glater, E. E., Megeath, L. J., Stowers, R. S. and Schwarz, T. L. (2006). "Axonal transport of mitochondria requires milton to recruit kinesin heavy chain and is light chain independent." J Cell Biol 173(4): 545-557.

Goldstein, L. S. and Yang, Z. (2000). "Microtubule-based transport systems in neurons: the roles of kinesins and dyneins." Annu Rev Neurosci 23: 39-71.

Guo, X., Macleod, G. T., Wellington, A., Hu, F., Panchumarthi, S., Schoenfield, M., Marin, L., Charlton, M. P., Atwood, H. L. and Zinsmaier, K. E. (2005). "The GTPase dMiro is required for axonal transport of mitochondria to Drosophila synapses." Neuron 47(3): 379-393.

Gurney, M. E., Pu, H., Chiu, A. Y., Dal Canto, M. C., Polchow, C. Y., Alexander, D. D., Caliendo, J., Hentati, A., Kwon, Y. W., Deng, H. X. and et al. (1994). "Motor neuron degeneration in mice that express a human Cu,Zn superoxide dismutase mutation." Science 264(5166): 1772-1775.

Habura, A., Tikhonenko, I., Chisholm, R. L. and Koonce, M. P. (1999). "Interaction mapping of a dynein heavy chain. Identification of dimerization and intermediate-chain binding domains." J Biol Chem 274(22): 15447-15453.

Hirokawa, N., Pfister, K. K., Yorifuji, H., Wagner, M. C., Brady, S. T. and Bloom, G. S. (1989). "Submolecular domains of bovine brain kinesin identified by electron microscopy and monoclonal antibody decoration." Cell 56(5): 867-878.

Hirokawa, N. and Takemura, R. (2005). "Molecular motors and mechanisms of directional transport in neurons." Nat Rev Neurosci 6(3): 201-214.

Hollenbeck, P. J. and Saxton, W. M. (2005). "The axonal transport of mitochondria." J Cell Sci 118(Pt 23): 5411-5419.

Hughes, S. M., Vaughan, K. T., Herskovits, J. S. and Vallee, R. B. (1995). "Molecular analysis of a cytoplasmic dynein light intermediate chain reveals homology to a family of ATPases." J Cell Sci 108 (Pt 1): 17-24.

Jellali, A., Metz-Boutigue, M. H., Surgucheva, I., Jancsik, V., Schwartz, C., Filliol, D., Gelfand, V. I. and Rendon, A. (1994). "Structural and biochemical properties of kinesin heavy chain associated with rat brain mitochondria." Cell Motil Cytoskeleton 28(1): 79-93.

King, S. J., Brown, C. L., Maier, K. C., Quintyne, N. J. and Schroer, T. A. (2003). "Analysis of the dynein-dynactin interaction in vitro and in vivo." Mol Biol Cell 14(12): 5089-5097.

King, S. J. and Schroer, T. A. (2000). "Dynactin increases the processivity of the cytoplasmic dynein motor." Nat Cell Biol 2(1): 20-24.

Kong, J. and Xu, Z. (1998). "Massive mitochondrial degeneration in motor neurons triggers the onset of amyotrophic lateral sclerosis in mice expressing a mutant SOD1." J Neurosci 18(9): 3241-3250.

Kristal, B. S. and Dubinsky, J. M. (1997). "Mitochondrial permeability transition in the central nervous system: induction by calcium cycling-dependent and -independent pathways." J Neurochem 69(2): 524-538.

Kwinter, D. M., Lo, K., Mafi, P. and Silverman, M. A. (2009). "Dynactin regulates bidirectional transport of dense-core vesicles in the axon and dendrites of cultured hippocampal neurons." Neuroscience 162(4): 1001-1010.

Labrousse, A. M., Zappaterra, M. D., Rube, D. A. and van der Bliek, A. M. (1999). "C. elegans dynamin-related protein DRP-1 controls severing of the mitochondrial outer membrane." Mol Cell 4(5): 815-826.

Landis, D. M., Hall, A. K., Weinstein, L. A. and Reese, T. S. (1988). "The organization of cytoplasm at the presynaptic active zone of a central nervous system synapse." Neuron 1(3): 201-209.

Lawson, V. H., Graham, B. V. and Flanigan, K. M. (2005). "Clinical and electrophysiologic features of CMT2A with mutations in the mitofusin 2 gene." Neurology 65(2): 197-204.

Lee, M. K., Xu, Z., Wong, P. C. and Cleveland, D. W. (1993). "Neurofilaments are obligate heteropolymers in vivo." J Cell Biol 122(6): 1337-1350.

Levy, J. R. and Holzbaur, E. L. (2006). "Cytoplasmic dynein/dynactin function and dysfunction in motor neurons." Int J Dev Neurosci 24(2-3): 103-111.

Liesa, M., Palacin, M. and Zorzano, A. (2009). "Mitochondrial dynamics in mammalian health and disease." Physiol Rev 89(3): 799-845.

Ligon, L. A. and Steward, O. (2000). "Movement of mitochondria in the axons and dendrites of cultured hippocampal neurons." J Comp Neurol 427(3): 340-350.

Ligon, L. A. and Steward, O. (2000). "Role of microtubules and actin filaments in the movement of mitochondria in the axons and dendrites of cultured hippocampal neurons." J Comp Neurol 427(3): 351-361.

Llopis, J., McCaffery, J. M., Miyawaki, A., Farquhar, M. G. and Tsien, R. Y. (1998). "Measurement of cytosolic, mitochondrial, and Golgi pH in single living cells with green fluorescent proteins." Proc Natl Acad Sci U S A 95(12): 6803-6808.

Lyons, D. A., Naylor, S. G., Mercurio, S., Dominguez, C. and Talbot, W. S. (2008). "KBP is essential for axonal structure, outgrowth and maintenance in zebrafish,

providing insight into the cellular basis of Goldberg-Shprintzen syndrome." Development 135(3): 599-608.

Malaiyandi, L. M., Honick, A. S., Rintoul, G. L., Wang, Q. J. and Reynolds, I. J. (2005). "Zn2+ inhibits mitochondrial movement in neurons by phosphatidylinositol 3-kinase activation." J Neurosci 25(41): 9507-9514.

Mallavarapu, A. and Mitchison, T. (1999). "Regulated actin cytoskeleton assembly at filopodium tips controls their extension and retraction." J Cell Biol 146(5): 1097-1106.

Margulis, L. and Bermudes, D. (1985). "Symbiosis as a mechanism of evolution: status of cell symbiosis theory." Symbiosis 1: 101-124.

Martin, R., Vaida, B., Bleher, R., Crispino, M. and Giuditta, A. (1998). "Protein synthesizing units in presynaptic and postsynaptic domains of squid neurons." J Cell Sci 111 (Pt 21): 3157-3166.

Mattson, M. P. (2003). "Excitotoxic and excitoprotective mechanisms: abundant targets for the prevention and treatment of neurodegenerative disorders." Neuromolecular Med 3(2): 65-94.

Mattson, M. P., Gleichmann, M. and Cheng, A. (2008). "Mitochondria in neuroplasticity and neurological disorders." Neuron 60(5): 748-766.

Miki, H., Setou, M., Kaneshiro, K. and Hirokawa, N. (2001). "All kinesin superfamily protein, KIF, genes in mouse and human." Proc Natl Acad Sci U S A 98(13): 7004-7011.

Mocz, G. and Gibbons, I. R. (2001). "Model for the motor component of dynein heavy chain based on homology to the AAA family of oligomeric ATPases." Structure 9(2): 93-103.

Nangaku, M., Sato-Yoshitake, R., Okada, Y., Noda, Y., Takemura, R., Yamazaki, H. and Hirokawa, N. (1994). "KIF1B, a novel microtubule plus end-directed monomeric motor protein for transport of mitochondria." Cell 79(7): 1209-1220.

Olichon, A., Baricault, L., Gas, N., Guillou, E., Valette, A., Belenguer, P. and Lenaers, G. (2003). "Loss of OPA1 perturbates the mitochondrial inner membrane structure and integrity, leading to cytochrome c release and apoptosis." J Biol Chem 278(10): 7743-7746.

Olney, J. W. and de Gubareff, T. (1978). "Glutamate neurotoxicity and Huntington's chorea." Nature 271(5645): 557-559.

Ong, L. L., Lim, A. P., Er, C. P., Kuznetsov, S. A. and Yu, H. (2000). "Kinectin-kinesin binding domains and their effects on organelle motility." J Biol Chem 275(42): 32854-32860.

Overly, C. C., Rieff, H. I. and Hollenbeck, P. J. (1996). "Organelle motility and metabolism in axons vs dendrites of cultured hippocampal neurons." J Cell Sci 109 (Pt 5): 971-980.

Palay, S. L. (1956). "Synapses in the central nervous system." J Biophys Biochem Cytol 2(4, Suppl): 193-202.

Pich, S., Bach, D., Briones, P., Liesa, M., Camps, M., Testar, X., Palacin, M. and Zorzano, A. (2005). "The Charcot-Marie-Tooth type 2A gene product, Mfn2, up-regulates fuel oxidation through expression of OXPHOS system." Hum Mol Genet 14(11): 1405-1415.

Povlishock, J. T. (1976). "The fine structure of the axons and growth cones of the human fetal cerebral cortex." Brain Res 114(3): 379-379i.

Quintyne, N. J., Gill, S. R., Eckley, D. M., Crego, C. L., Compton, D. A. and Schroer, T. A. (1999). "Dynactin is required for microtubule anchoring at centrosomes." J Cell Biol 147(2): 321-334.

Quintyne, N. J. and Schroer, T. A. (2002). "Distinct cell cycle-dependent roles for dynactin and dynein at centrosomes." J Cell Biol 159(2): 245-254.

Reynolds, I. J. and Hastings, T. G. (1995). "Glutamate induces the production of reactive oxygen species in cultured forebrain neurons following NMDA receptor activation." J Neurosci 15(5 Pt 1): 3318-3327.

Rintoul, G. L. and Baimbridge, K. G. (2003). "Effects of calcium buffers and calbindin-D28k upon histamine-induced calcium oscillations and calcium waves in HeLa cells." Cell Calcium 34(2): 131-144.

Rintoul, G. L., Bennett, V. J., Papaconstandinou, N. A. and Reynolds, I. J. (2006). "Nitric oxide inhibits mitochondrial movement in forebrain neurons associated with disruption of mitochondrial membrane potential." J Neurochem 97(3): 800-806.

Rintoul, G. L., Filiano, A. J., Brocard, J. B., Kress, G. J. and Reynolds, I. J. (2003). "Glutamate decreases mitochondrial size and movement in primary forebrain neurons." J Neurosci 23(21): 7881-7888.

Rintoul, G. L. and Reynolds, I. J. (2009). "Mitochondrial trafficking and morphology in neuronal injury." Biochim Biophys Acta.

Samso, M., Radermacher, M., Frank, J. and Koonce, M. P. (1998). "Structural characterization of a dynein motor domain." J Mol Biol 276(5): 927-937.

Santama, N., Er, C. P., Ong, L. L. and Yu, H. (2004). "Distribution and functions of kinectin isoforms." J Cell Sci 117(Pt 19): 4537-4549.

Santel, A. and Fuller, M. T. (2001). "Control of mitochondrial morphology by a human mitofusin." J Cell Sci 114(Pt 5): 867-874.

Schafer, D. A., Gill, S. R., Cooper, J. A., Heuser, J. E. and Schroer, T. A. (1994). "Ultrastructural analysis of the dynactin complex: an actin-related protein is a component of a filament that resembles F-actin." J Cell Biol 126(2): 403-412.

Schnapp, B. J. and Reese, T. S. (1989). "Dynein is the motor for retrograde axonal transport of organelles." Proc Natl Acad Sci U S A 86(5): 1548-1552.

Schroer, T. A. (2004). "Dynactin." Annu Rev Cell Dev Biol 20: 759-779.

Skulachev, V. P. (2001). "Mitochondrial filaments and clusters as intracellular power-transmitting cables." Trends Biochem Sci 26(1): 23-29.

Smirnova, E., Shurland, D. L., Ryazantsev, S. N. and van der Bliek, A. M. (1998). "A human dynamin-related protein controls the distribution of mitochondria." J Cell Biol 143(2): 351-358.

Song, Z., Chen, H., Fiket, M., Alexander, C. and Chan, D. C. (2007). "OPA1 processing controls mitochondrial fusion and is regulated by mRNA splicing, membrane potential, and Yme1L." J Cell Biol 178(5): 749-755.

Song, Z., Ghochani, M., McCaffery, J. M., Frey, T. G. and Chan, D. C. (2009). "Mitofusins and OPA1 mediate sequential steps in mitochondrial membrane fusion." Mol Biol Cell 20(15): 3525-3532.

Stout, A. K., Raphael, H. M., Kanterewicz, B. I., Klann, E. and Reynolds, I. J. (1998). "Glutamate-induced neuron death requires mitochondrial calcium uptake." Nat Neurosci 1(5): 366-373.

Waterman-Storer, C. M., Karki, S. and Holzbaur, E. L. (1995). "The p150Glued component of the dynactin complex binds to both microtubules and the actin-related protein centractin (Arp-1)." Proc Natl Acad Sci U S A 92(5): 1634-1638.

White, R. J. and Reynolds, I. J. (1996). "Mitochondrial depolarization in glutamate-stimulated neurons: an early signal specific to excitotoxin exposure." J Neurosci 16(18): 5688-5697.

Wozniak, M. J., Melzer, M., Dorner, C., Haring, H. U. and Lammers, R. (2005). "The novel protein KBP regulates mitochondria localization by interaction with a kinesin-like protein." BMC Cell Biol 6: 35.

Zanelli, S. A., Trimmer, P. A. and Solenski, N. J. (2006). "Nitric oxide impairs mitochondrial movement in cortical neurons during hypoxia." J Neurochem 97(3): 724-736.

Zinsmaier, K. E., Babic, M. and Russo, G. J. (2009). "Mitochondrial transport dynamics in axons and dendrites." Results Probl Cell Differ 48: 107-139.